

# Snowflake Divertor Experiments on TCV

**Francesco PIRAS**

S.Coda, B.P.Duval, B.Labit, J.Marki, S.Yu.Medvedev,  
J-M.Moret, A.Pitzschke, O.Sauter and the TCV team

**Centre de Recherches en Physique des Plasmas  
Ecole Polytechnique Fédérale de Lausanne, Switzerland**

**presented at Princeton Plasma Physics Laboratory**

# Outline of the Talk

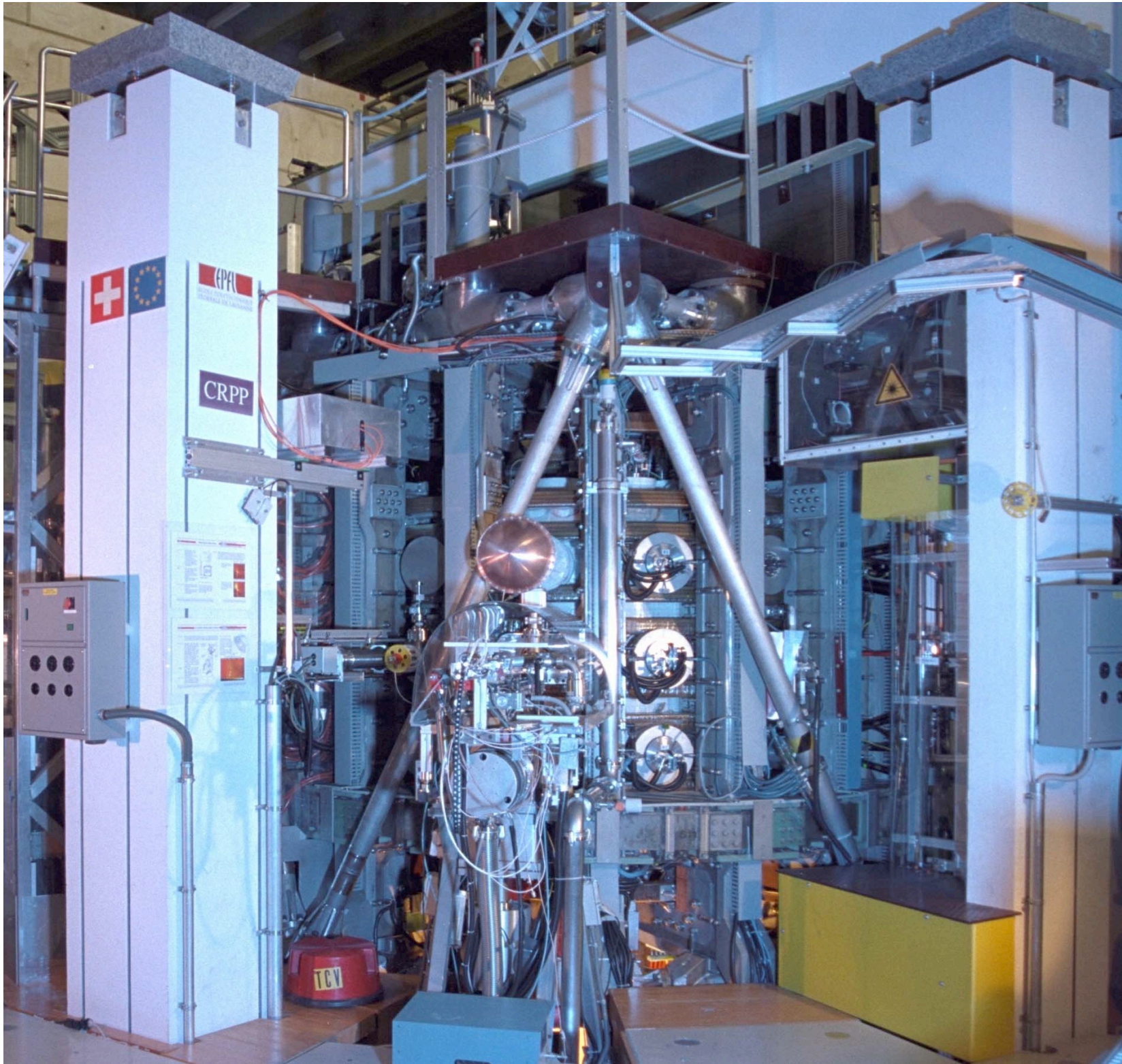
- The TCV Tokamak
- Magnetic in-situ Calibration
- Ohmic and Assisted Plasma Start-up
- Doublet Shaped Plasmas
- Snowflake Divertor
  - ▶ Snowflake divertor on TCV
  - ▶ Magnetic properties of the TCV snowflake
  - ▶ Snowflake divertor in the H-mode regime

# The TCV Tokamak



# TCV - Tokamak à Configuration Variable

## Mission



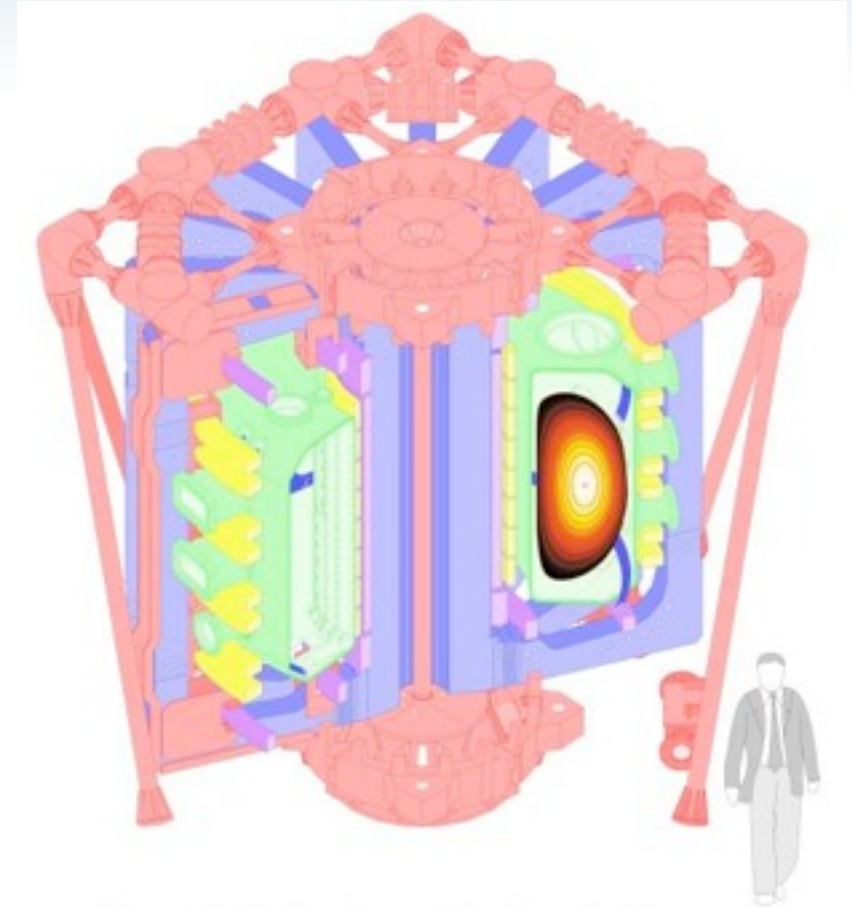
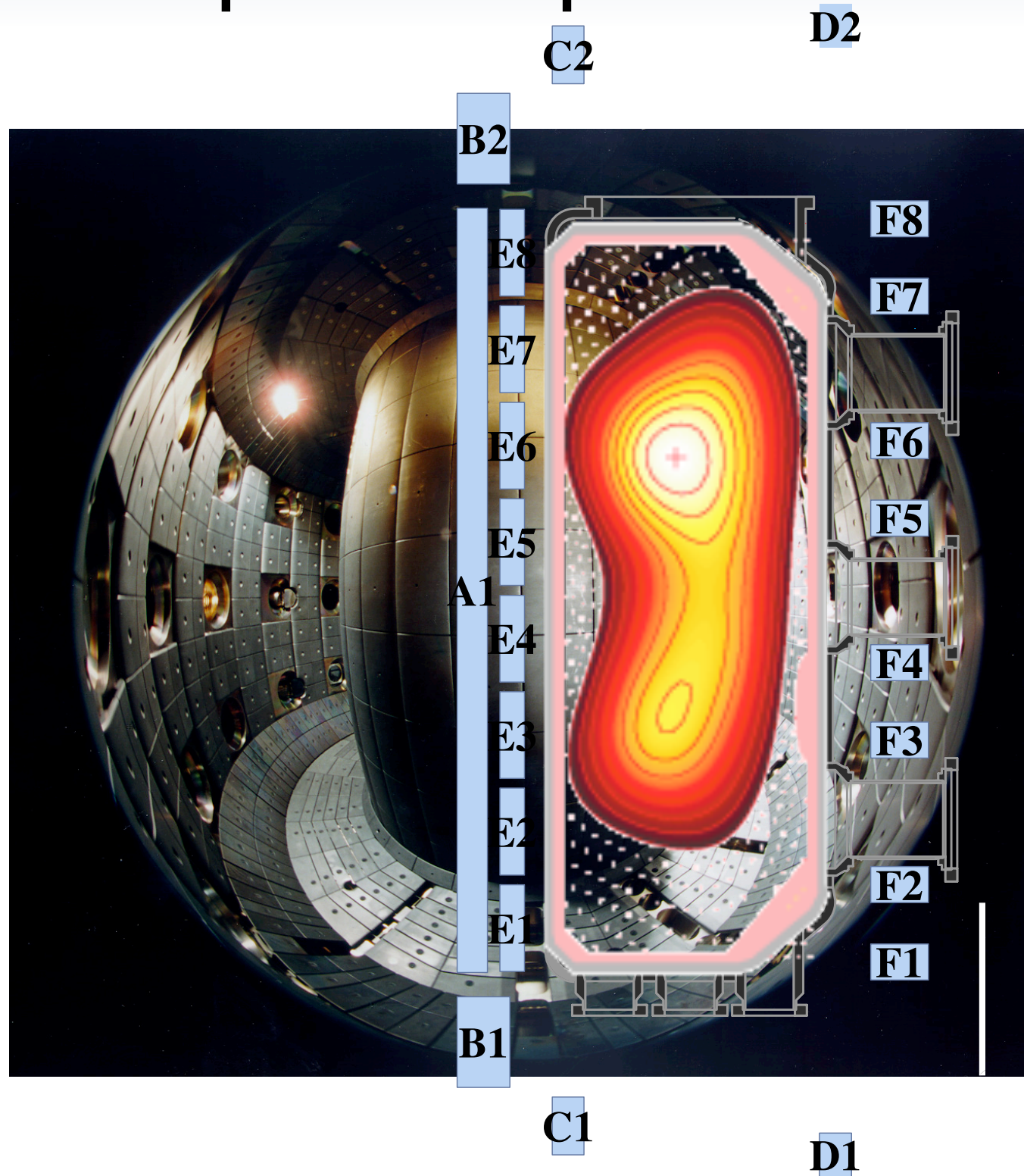
## Contribute to physics basis for

- ITER scenarios
- DEMO design
- Tokamak concept improvement



# Unique TCV Features

## Flexible plasma shapes



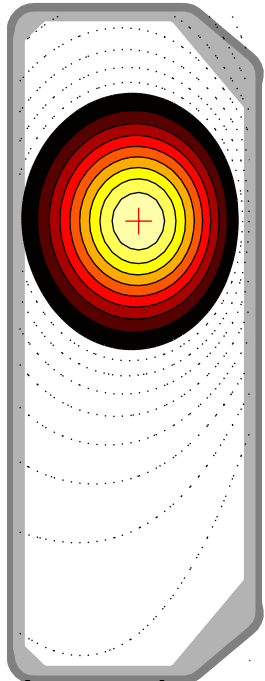
### ○ TCV Parameters

- $R = 0.88\text{m}; a = 0.25\text{m}$
- $B_T \leq 1.5\text{T}; I_p \leq 1.2\text{MA}$
- $0.9 \leq \text{elongation } \kappa \leq 2.8$
- $-0.8 \leq \text{triangularity } \delta \leq 0.9$
- Internal fast  $n=0$  coils  
(as in ITER)

# Unique TCV Features

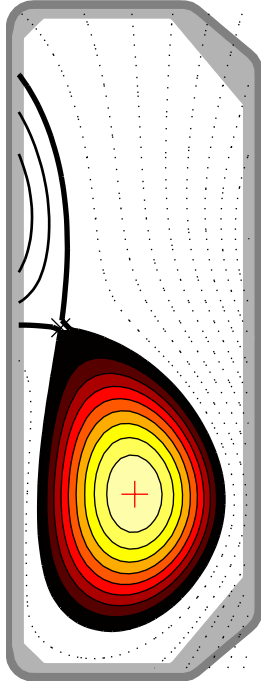
## Flexible plasma shapes

#9849 - 0.5s



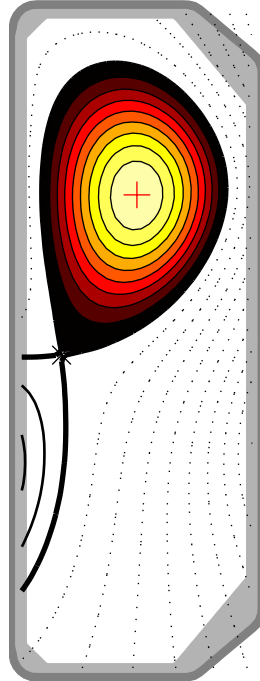
Limited  
 $\delta=0$  -  $I_p=230\text{kA}$   
 #18548 - 1.5s

#6010 - 0.8s



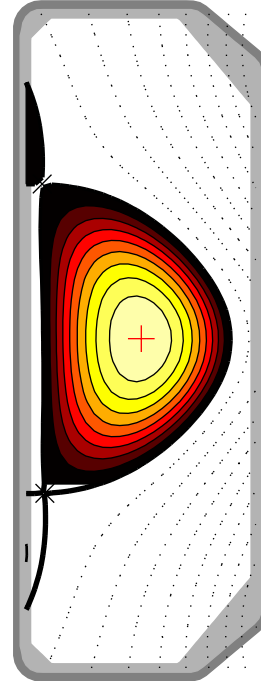
SN upper  
 $I_p=330\text{kA}$   
 #6442 - 0.5s

#5650 - 0.8s



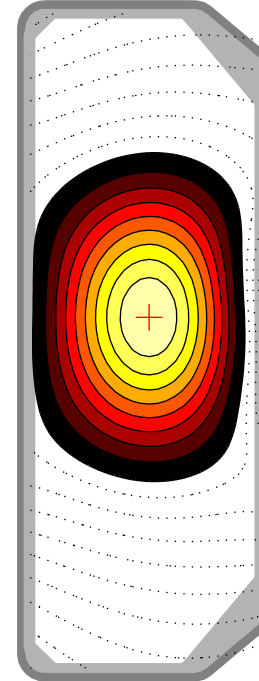
SN lower  
 $I_p=335\text{kA}$   
 #10159 - 0.01s

#8856 - 0.29s



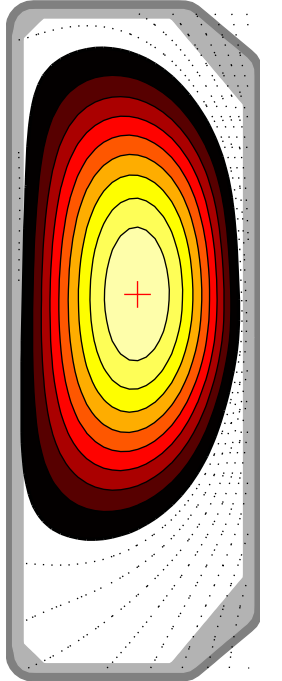
DN  
 $I_p=325\text{kA}$   
 #19373 - 0.42s

#11962 - 1s

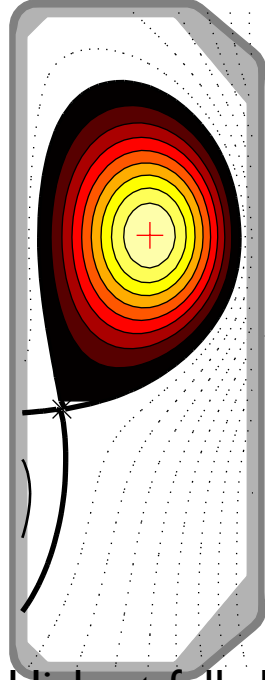


Highest squareness  
 $\lambda=0.5$   
 #11928 - 0.67s

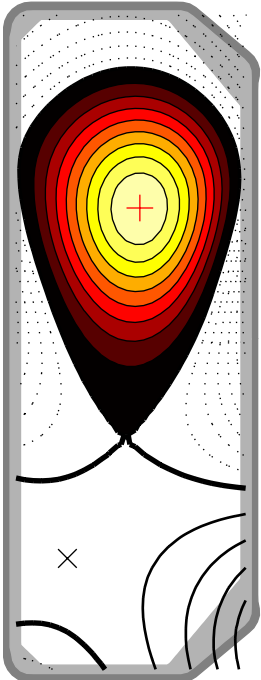
#11368 - 0.65s



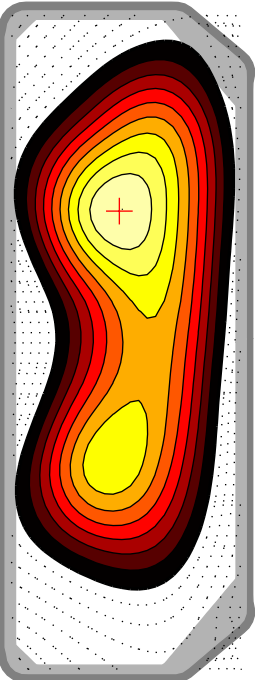
Highest current  
 $I_p=1.06\text{MA}$   
 #36151 - 0.457s



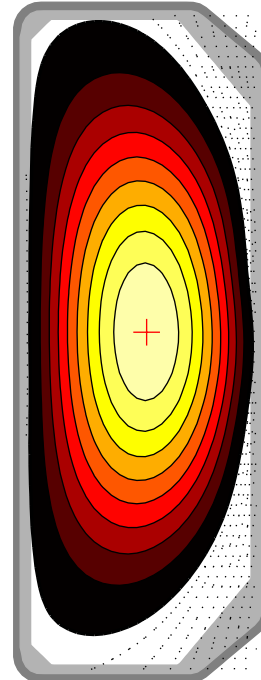
Highest fully ECCD  
 driven current  
 $I_p=210\text{kA}$



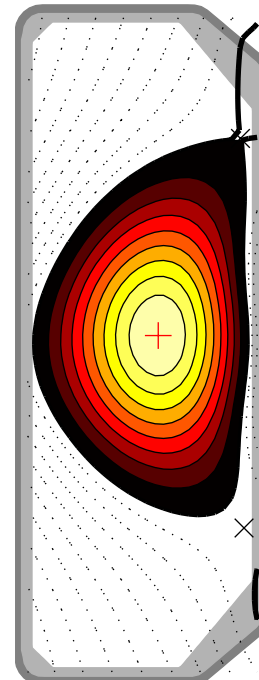
Pear shape  
 $I_p=360\text{kA}$



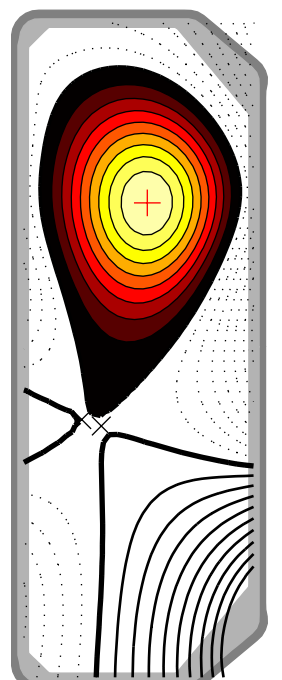
Doublet shape  
 $I_p=115\text{kA}$



Highest elongation  
 $k=2.8$



Lowest triangularity  
 $\delta=-0.77$

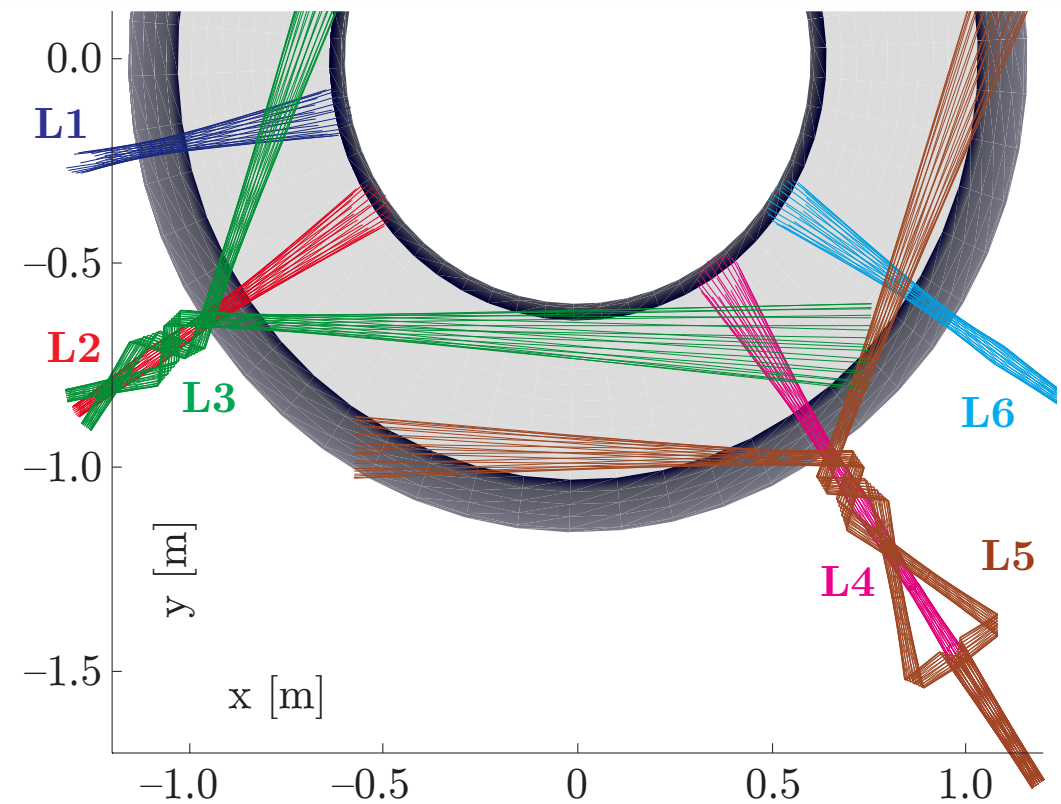
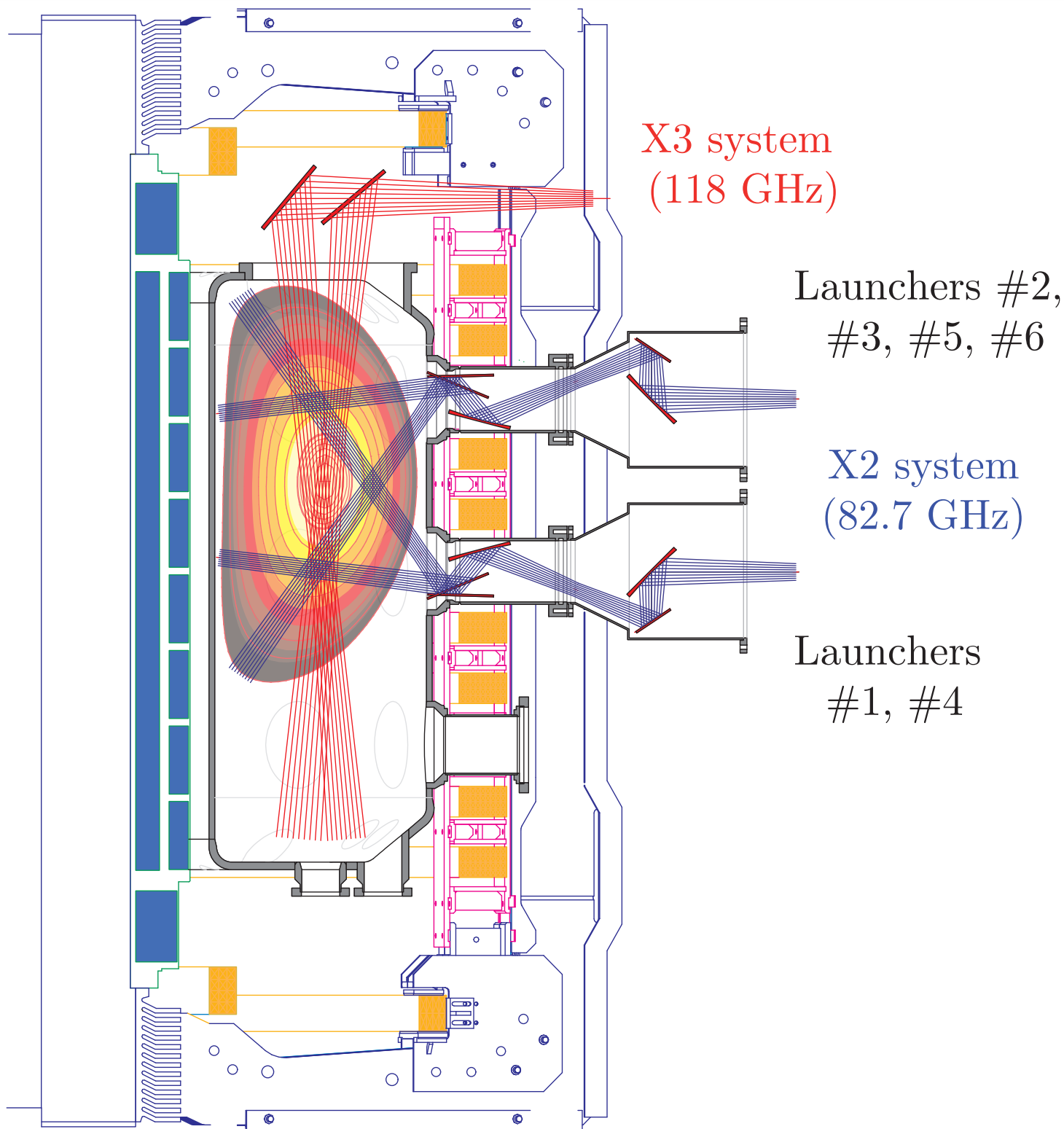


Snowflake  
 $I_p=230\text{kA}$



# Unique TCV Features

## Electron Cyclotron Systems



- **2<sup>nd</sup> harmonic X2 (82.7GHz)**  
6 × 0.5MW - 2s  
Side launch ECH, ECCD  
 $n_{\text{cut-off}} = 4 \times 10^{19} \text{m}^{-3}$
- **3<sup>rd</sup> harmonic X3 (118GHz)**  
3 × 0.5MW - 2s  
Top launch ECH  
 $n_{\text{cut-off}} \approx 10^{20} \text{m}^{-3}$



# Magnetics in-situ Calibration

# Magnetics in-situ Calibration

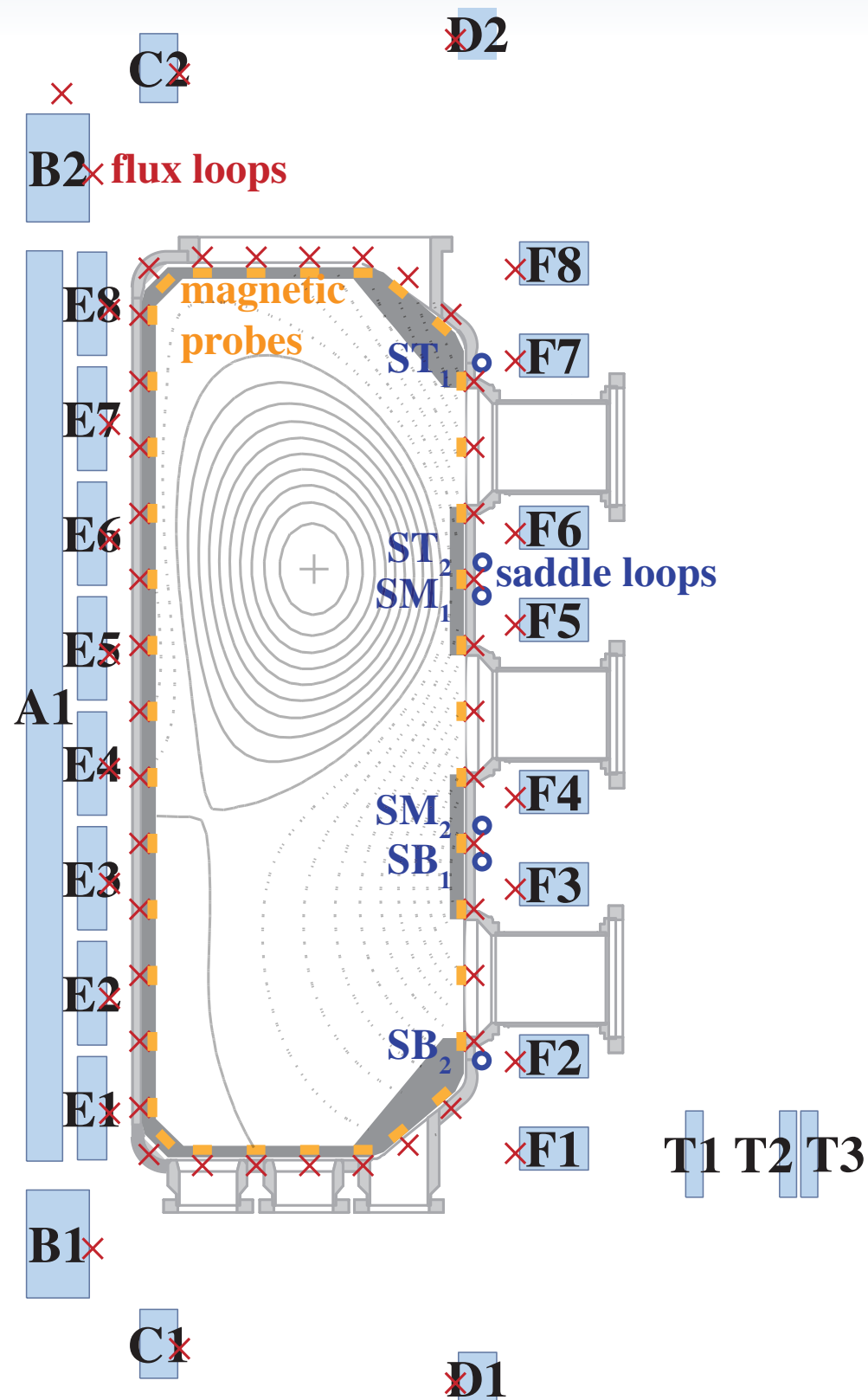
## Motivation

- Axisymmetric errors ( $n = 0$ ):
  - ▶ Plasma shape deformation
  - ▶ Wrong plasma position/strike points location
  - ▶ Caused by:
    - Errors in the radius and vertical position of the PF coils
    - Errors in the measured PF coil currents
- Asymmetric errors ( $n > 0$ ):
  - ▶ Creation of magnetic islands
  - ▶ Locked modes
  - ▶ Caused by:
    - Misalignment/deformation of the PF coils

## Goal of the calibration

- Find the real positions and gains of the TCV magnetic system

# The TCV Magnetic System



- ▶ 16 PF Coils (E and F)
- ▶ 7 ohmic coils (A, B, C and D)
- ▶ 3 toroidal field connections (T)
- ▶ 4 x 38 magnetic field probes
- ▶ 61 flux loops
- ▶ 24 saddle loops



# The Calibration Technique

- Each coil is separately powered
- All magnetic signals are acquired and compared to expected values

$$\Delta \Psi_f = \Psi_f - \underline{\underline{\mathbf{M}}}_{fc} \mathbf{I}_c$$

$$\Delta \mathbf{b}_m = \mathbf{b}_m - \underline{\underline{\mathbf{B}}}_{mc} \mathbf{I}_c$$

$$\Delta \Psi_s = \Psi_s - \underline{\underline{\mathbf{M}}}_{sc} \mathbf{I}_c$$

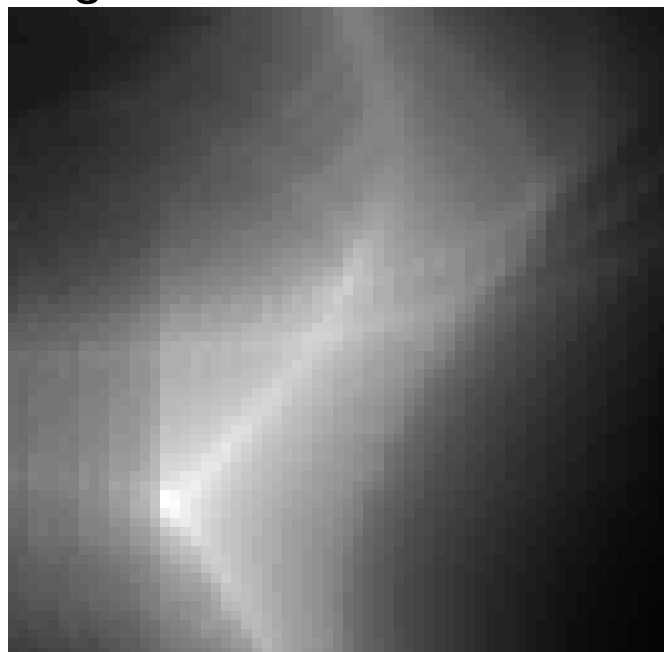
- The discrepancies are associated to calibration errors (660 parameters)
- The correction parameters are determined by minimizing a cost function
  
- The error on the PF coils position is of the order of ~1 mm
- The error on the  $n = 0$  poloidal field is ~1 mT
- The  $n = 1$  error field is of ~0.1 mT

# Ohmic and Assisted Plasma Start-up

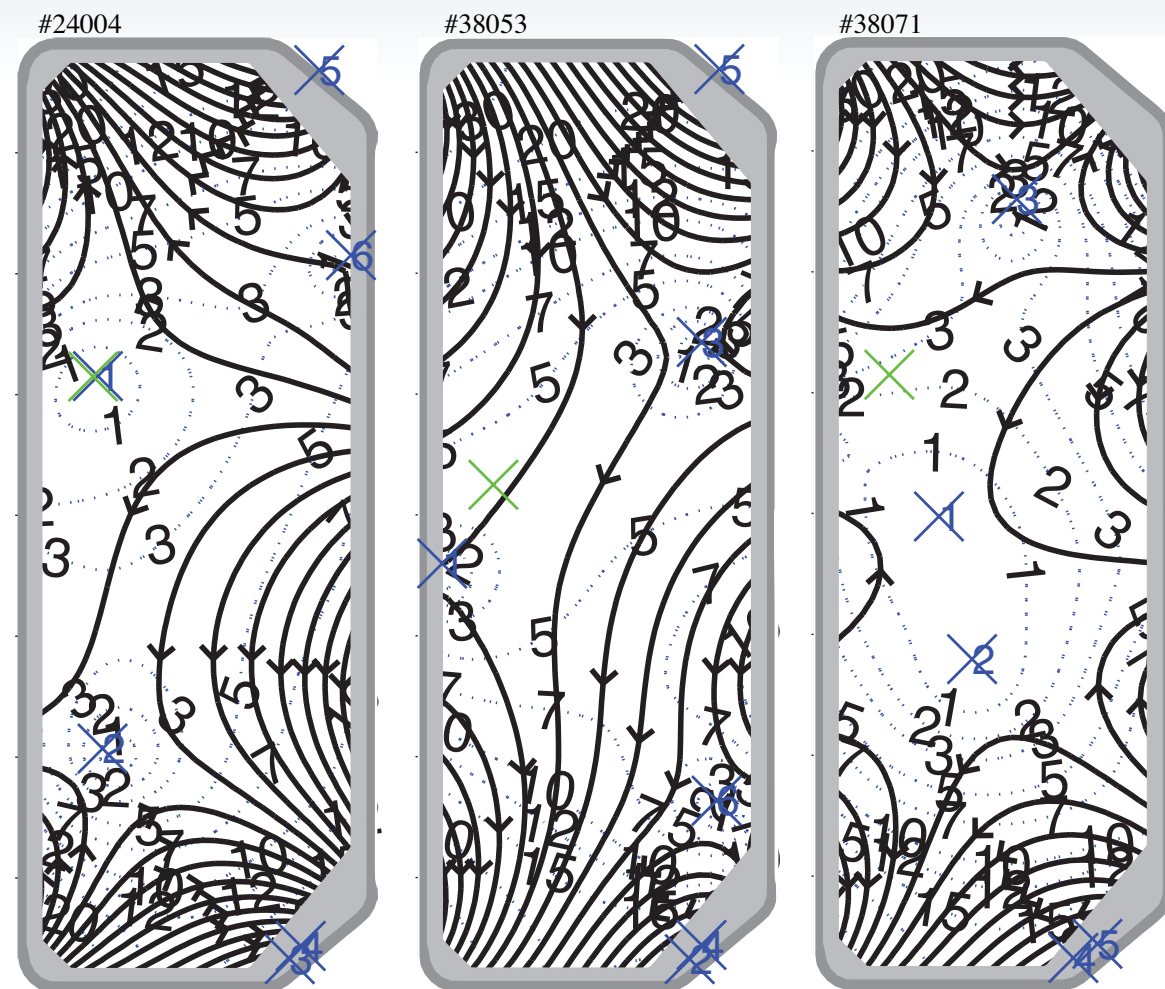
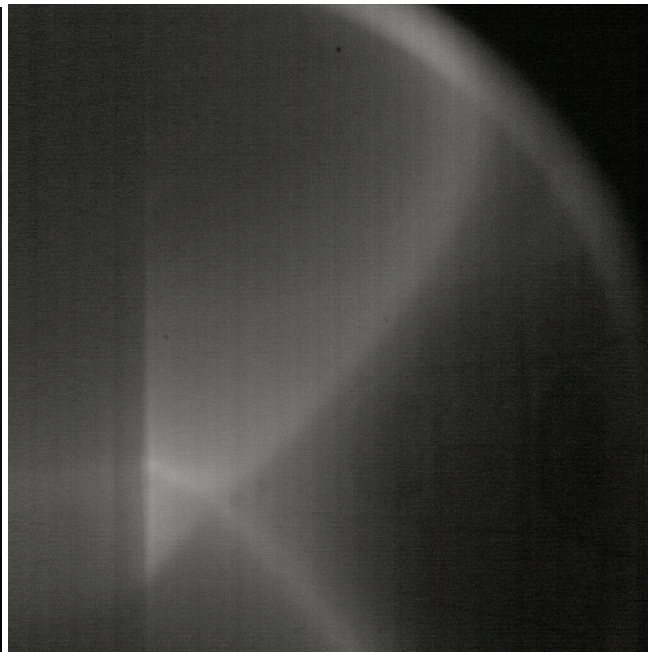
# Ohmic Plasma Start-up

- Start-up magnetic field reconstruction
- Plasma evolution during early ramp-up phase
- Statistical analysis of breakdown
- Modeling of the ohmic start-up

mag. rec.



camera



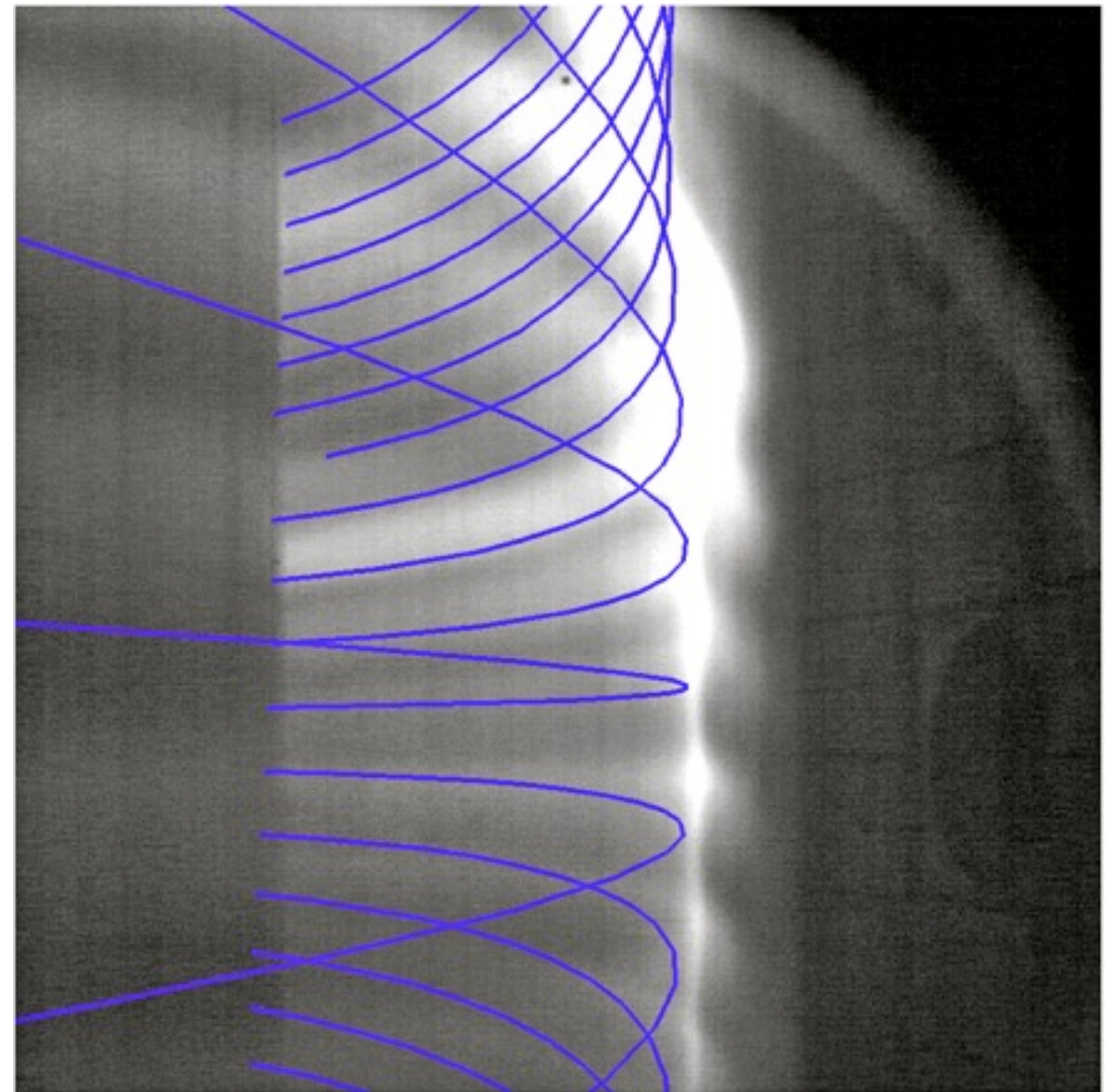
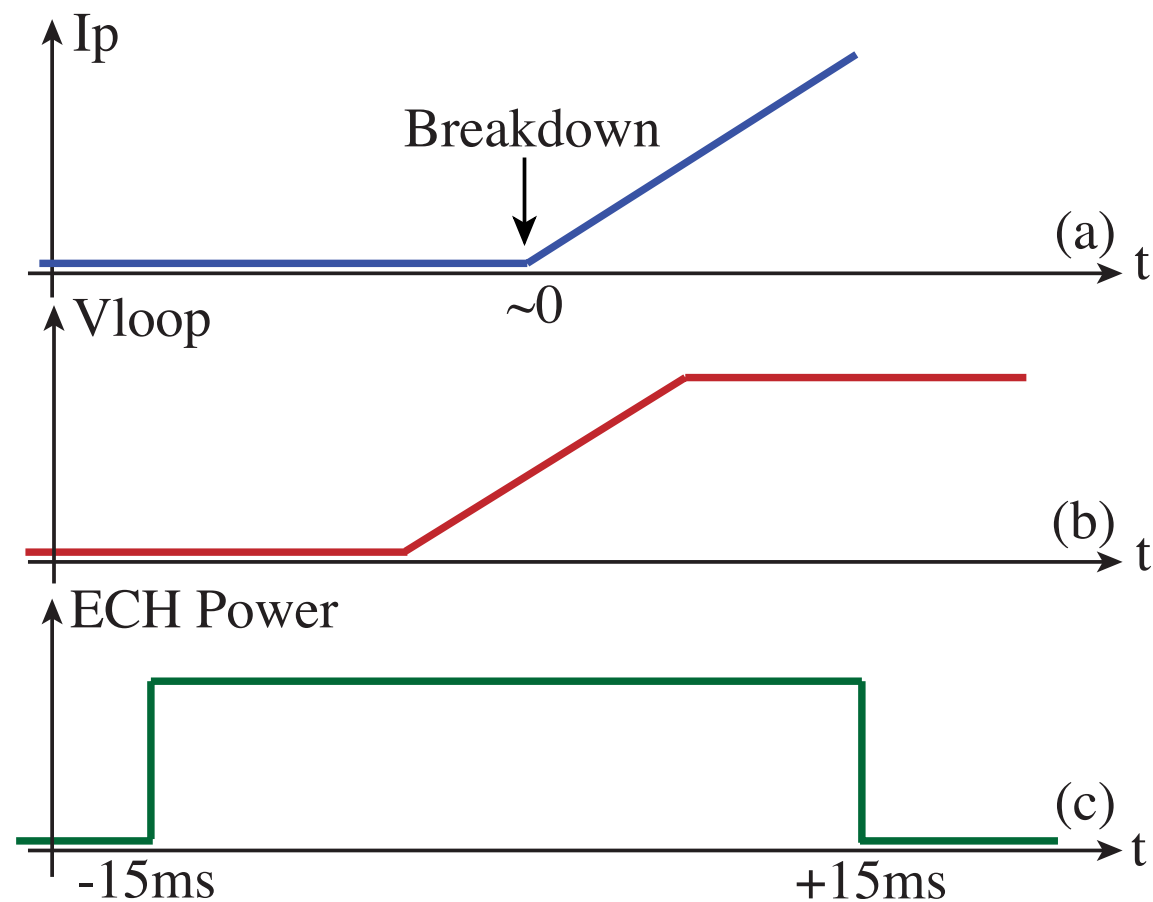
$$P_{i,j} = \int 1(R_{i,j}(t), Z_{i,j}(t)) dt$$

F.Piras, to be published



# Assisted ECH-X2 Plasma Start-up

- Assisted plasma start-up scenario



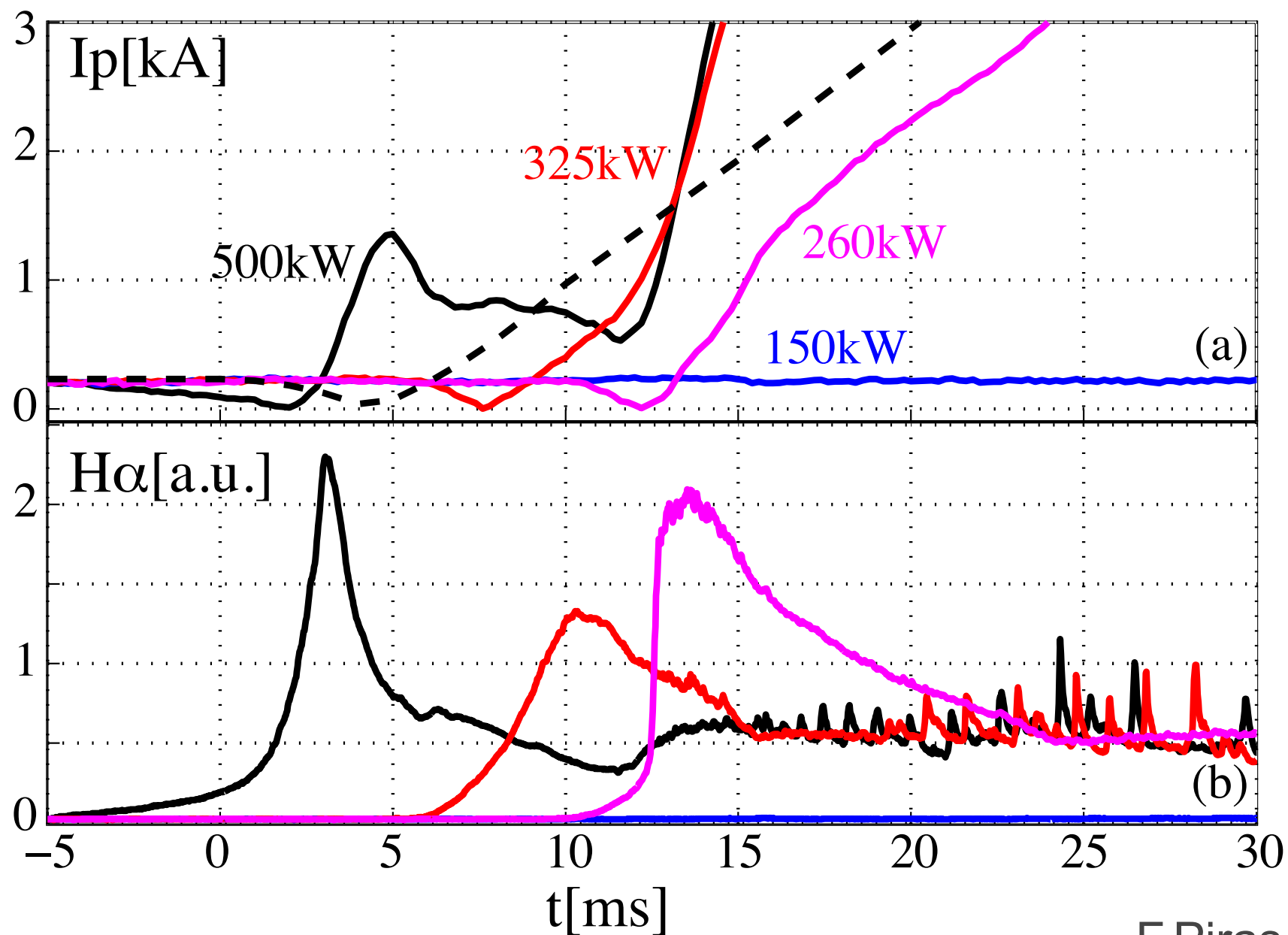
- Power injected from the LFS (central port)

F.Piras, to be published

# Assisted ECH-X2 Plasma Start-up

## Scan of the main ECH parameters

- ECH power scan (better high power)

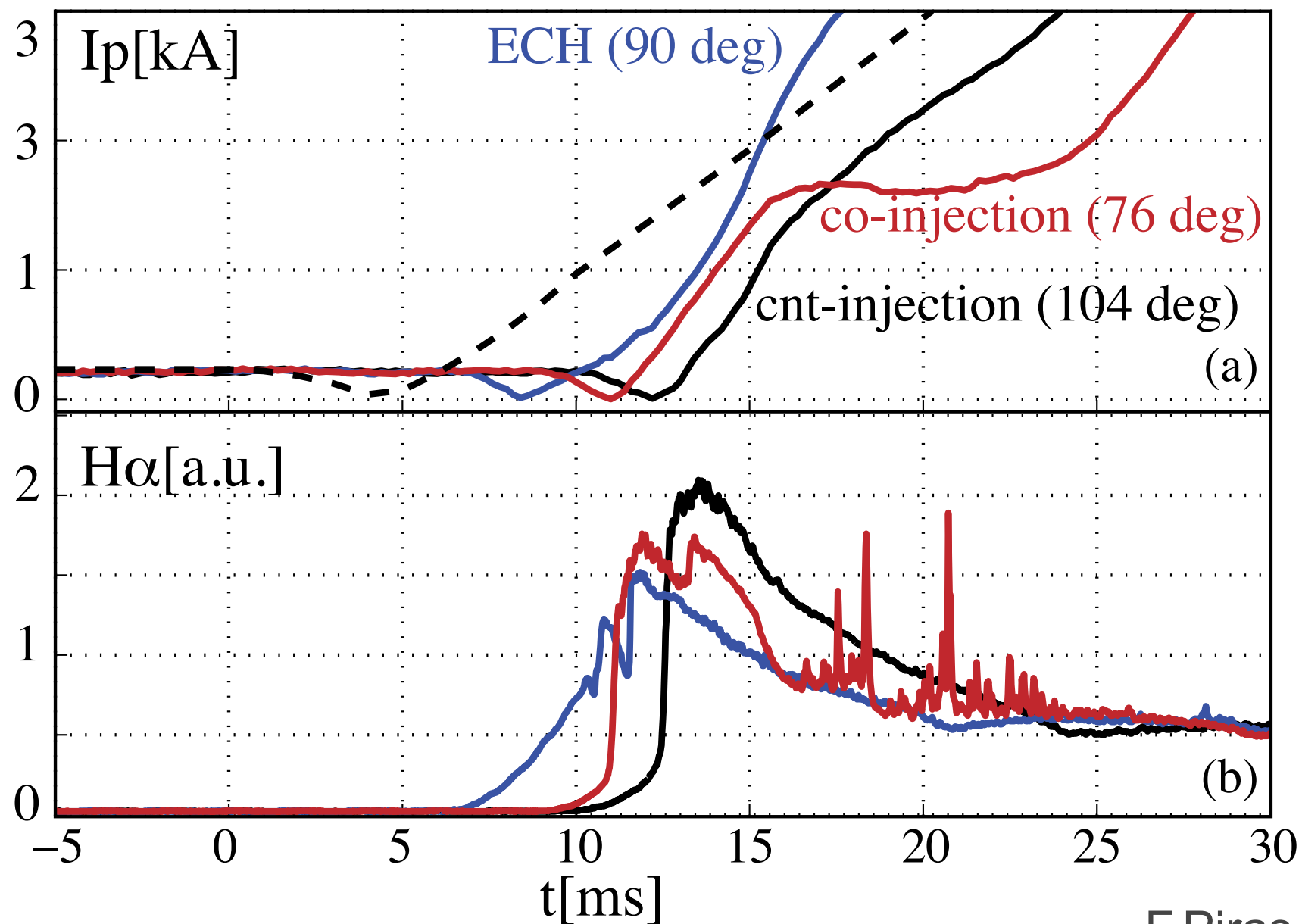


F.Piras, to be published

# Assisted ECH-X2 Plasma Start-up

## Scan of the main ECH parameters

- ECH toroidal angle scan (best 90 deg)



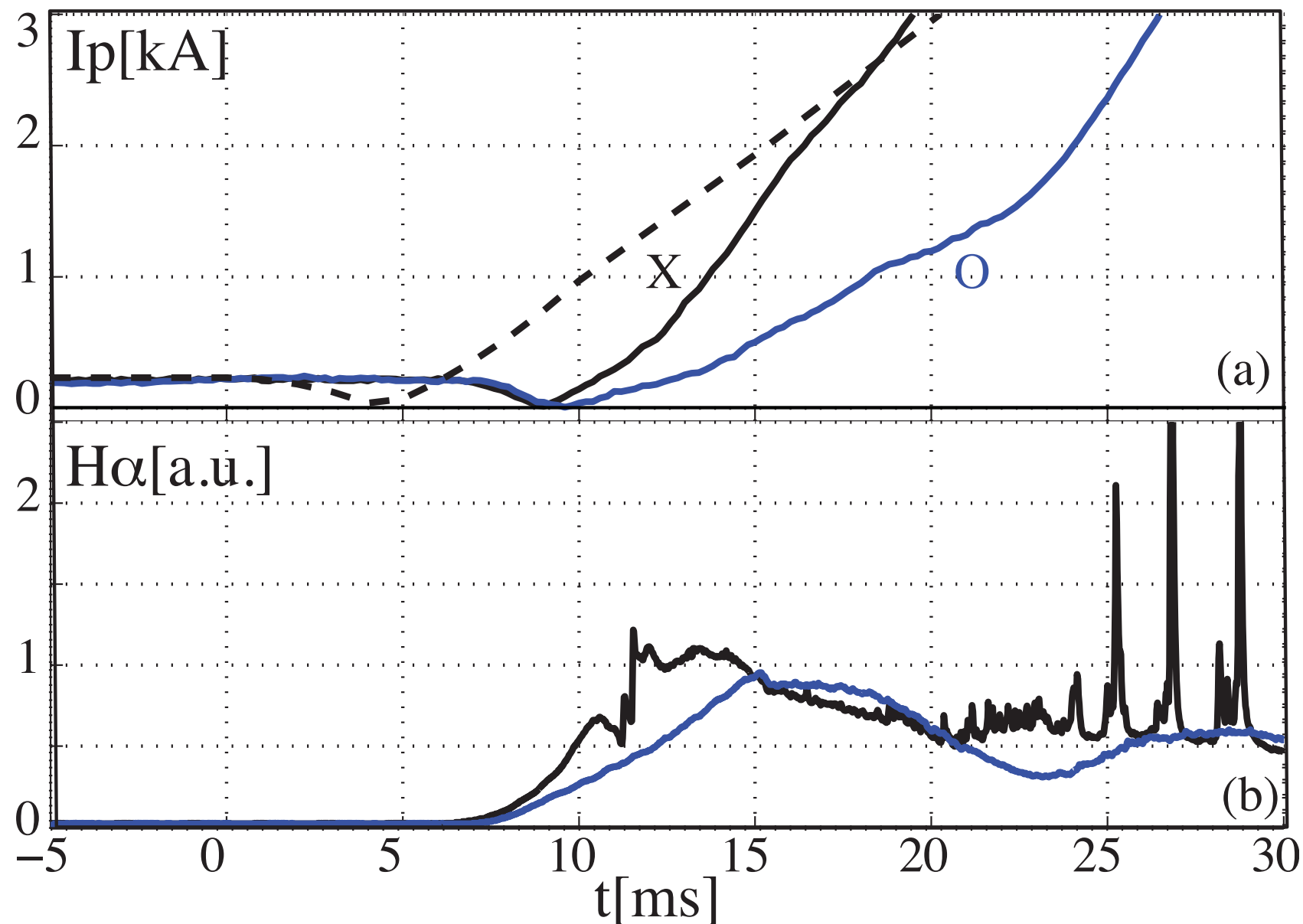
F.Piras, to be published



# Assisted ECH-X2 Plasma Start-up

## Scan of the main ECH parameters

- ECH polarization scan (better X pol.)



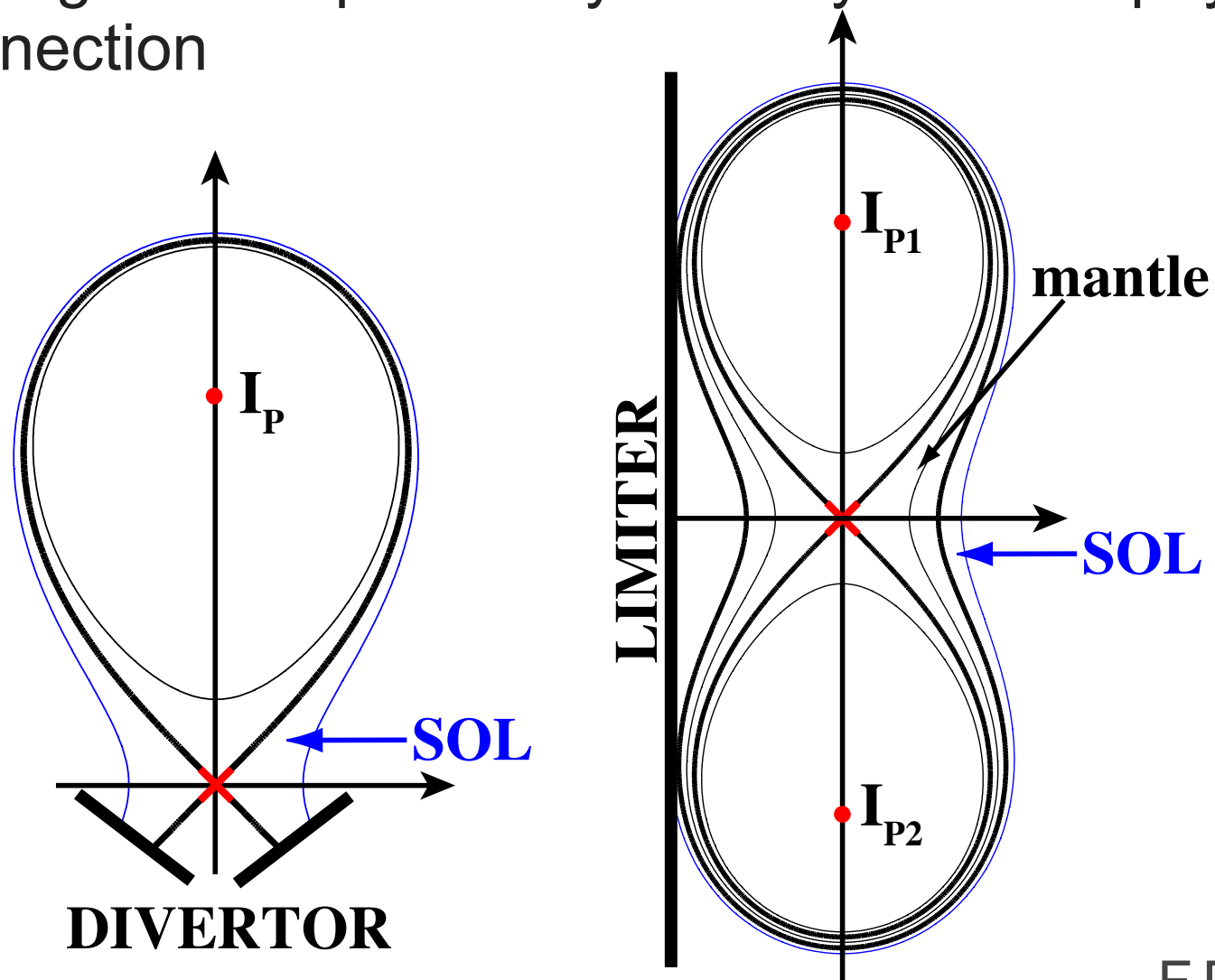
F.Piras, to be published

# Doublet Shaped Plasmas

# Doublet Shaped Plasma Concept

## Why doublets

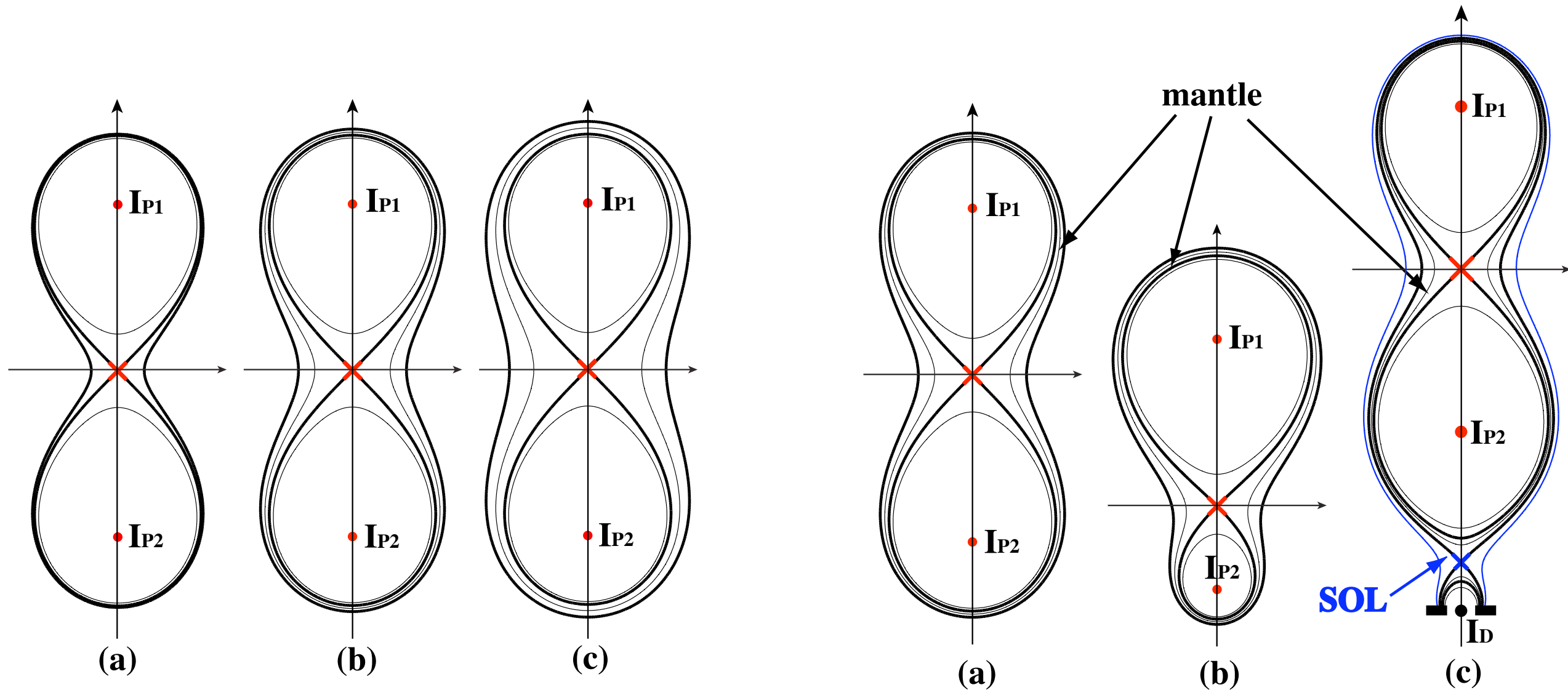
- Intrinsic zone of negative magnetic shear
  - Lower vertical instability growth rate
  - Possible advantages related to radioactive mantle
  - Net current present at the plasma pedestal
- 
- Doublet plasmas gives the possibility to study H-mode physics and magnetic reconnection



F.Piras, to be published

# Possible Doublet Configurations

Changing the mantle thickness, symmetry and edge properties

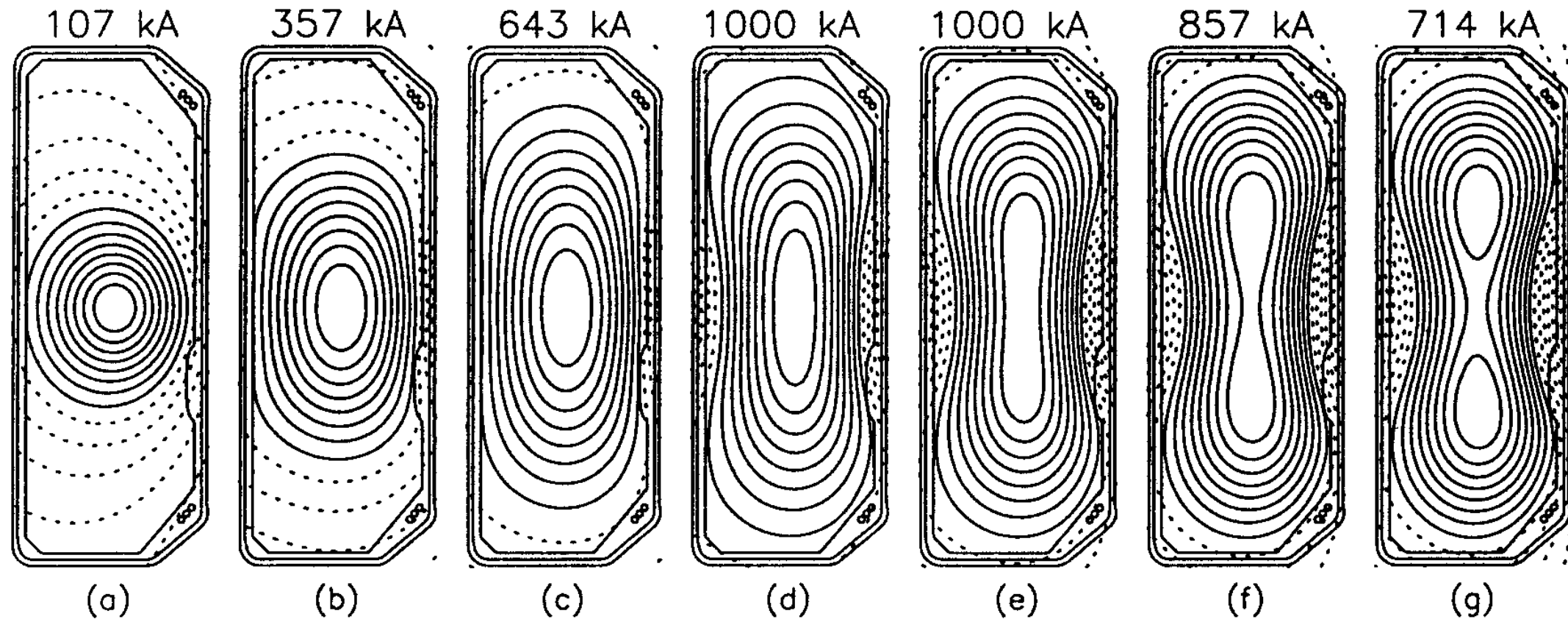


F.Piras, to be published



# Doublet Shaped Plasma Scenario

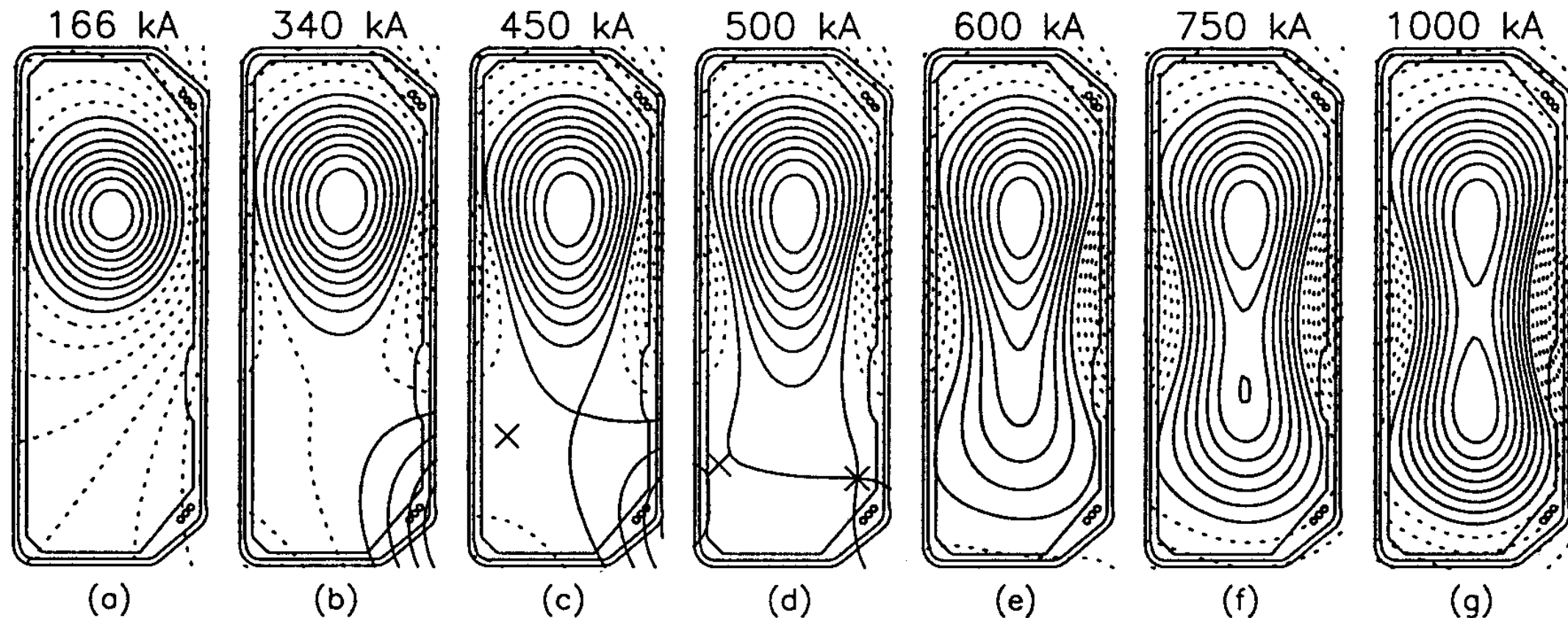
- Lateral constriction of highly elongated plasma



- Predicted maximum growth rate beyond ideal stability limit

# Doublet Shaped Plasma Scenario

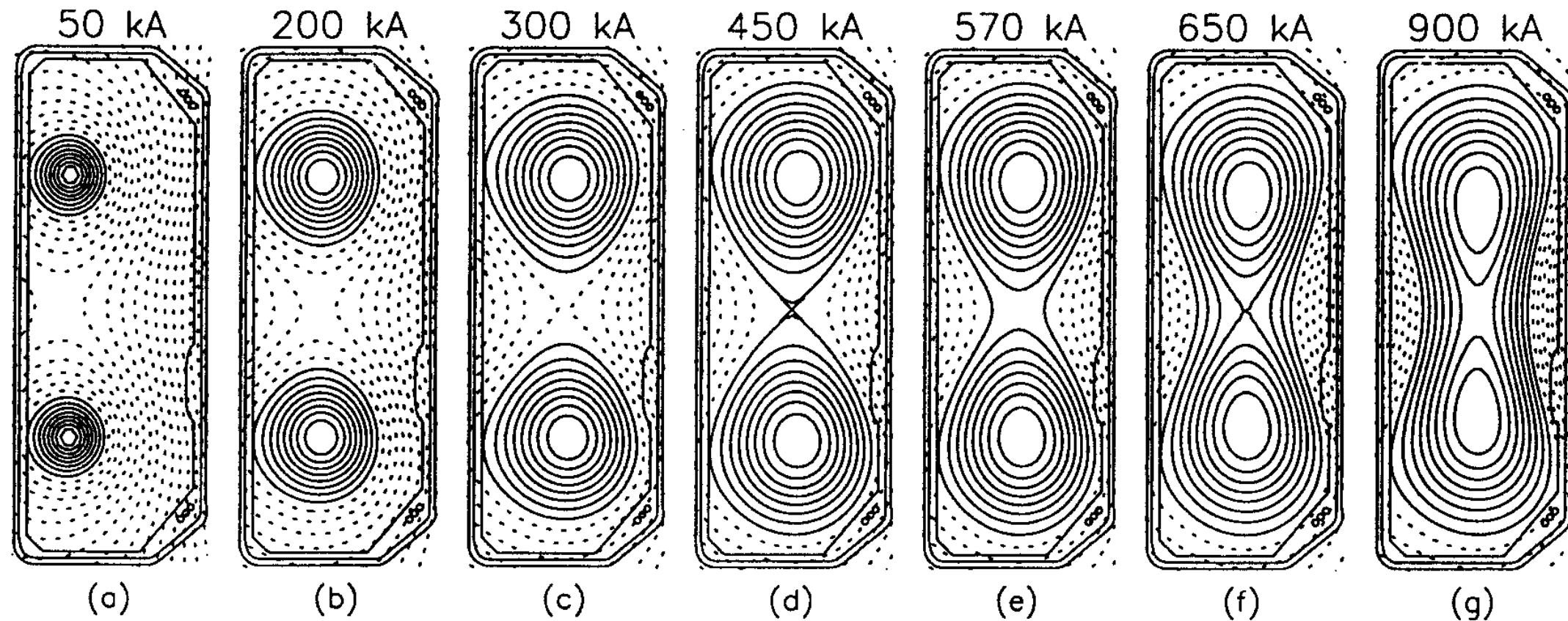
- Hour-glass scenario



- For peaked profiles the highly asymmetric doublets (e) does not exist
- Low MHD stability

# Doublet Shaped Plasma Scenario

- Merging of two droplet-shaped plasmas

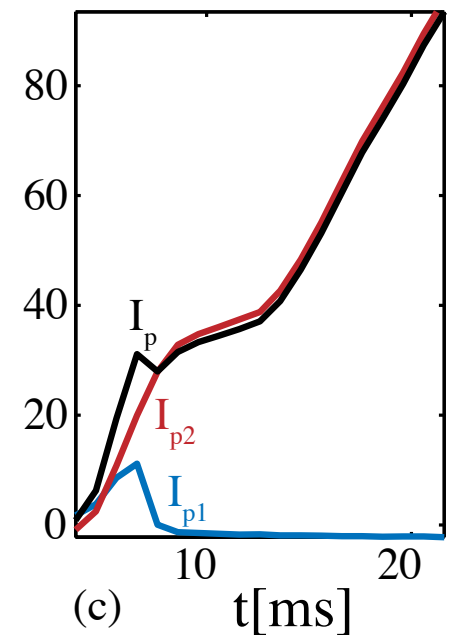
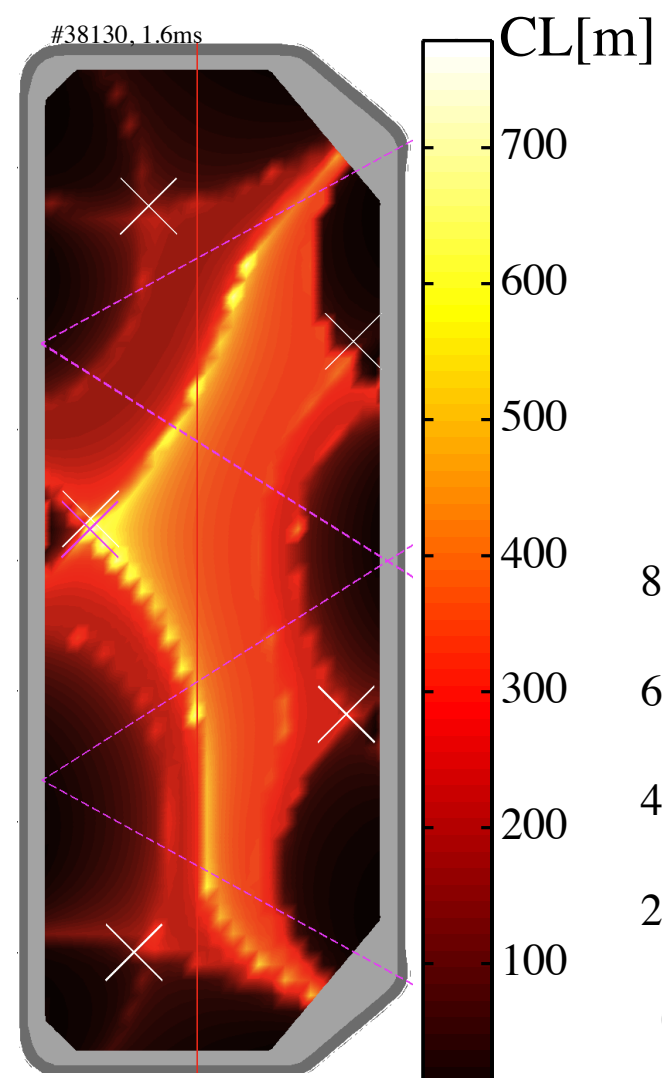
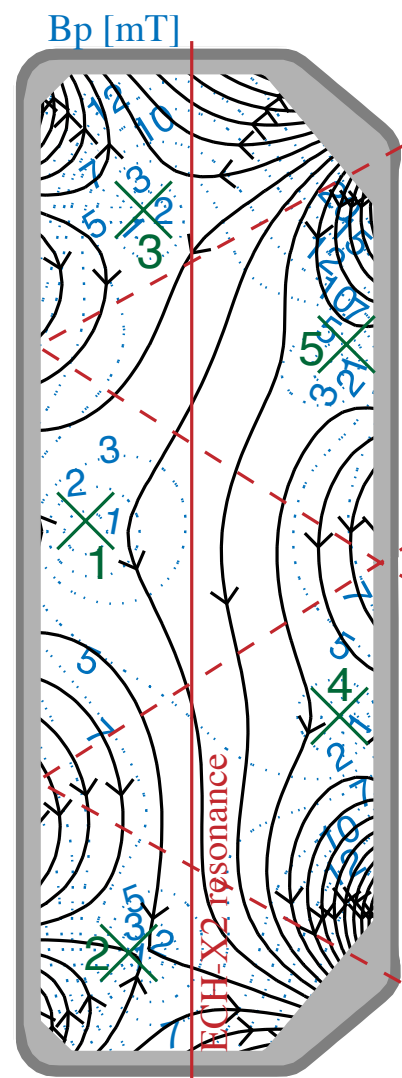
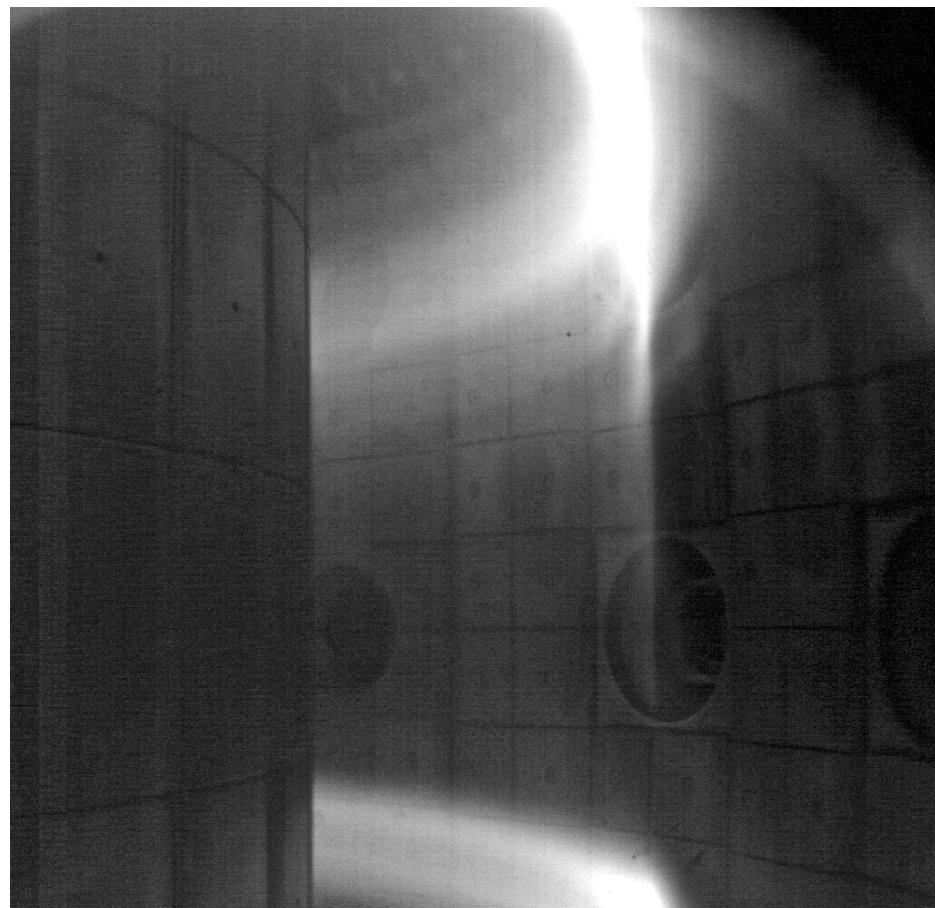


- The two breakdowns have to be simultaneous



# The Double Breakdown Problem

- Low chance to have a double ohmic breakdown
- Double breakdown assisted with ECH-X2



F.Piras, to be published

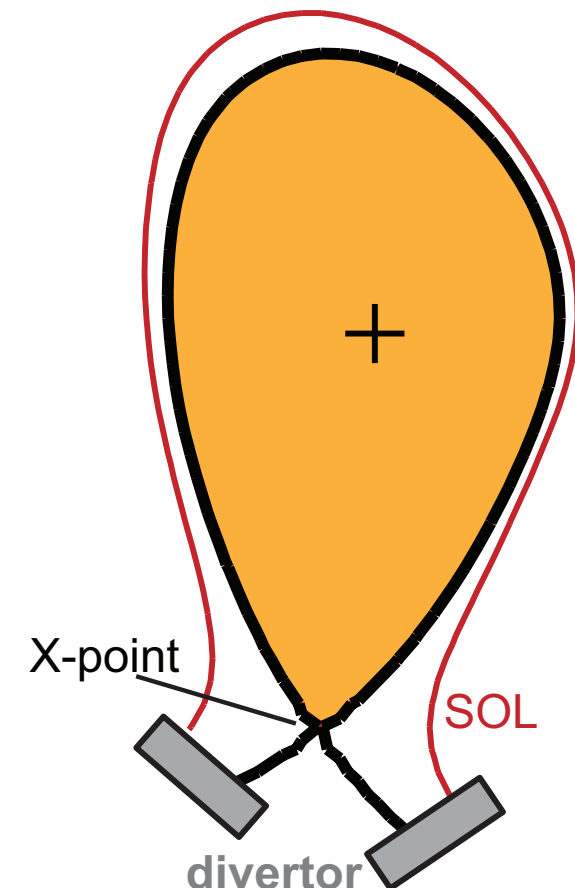
# Snowflake Divertor



# The Standard Divertor Configuration

Heat flux on the tokamak PFCs is a primary challenge of magnetic fusion research

- In diverted plasmas:
  - ▶ Magnetic X-point present ( $B_P = 0$ )
- Several strategies reduce the divertor heat loads:
  - ▶ Tile tilting
  - ▶ High flux expansion at strike points
  - ▶ Large radiated power fraction



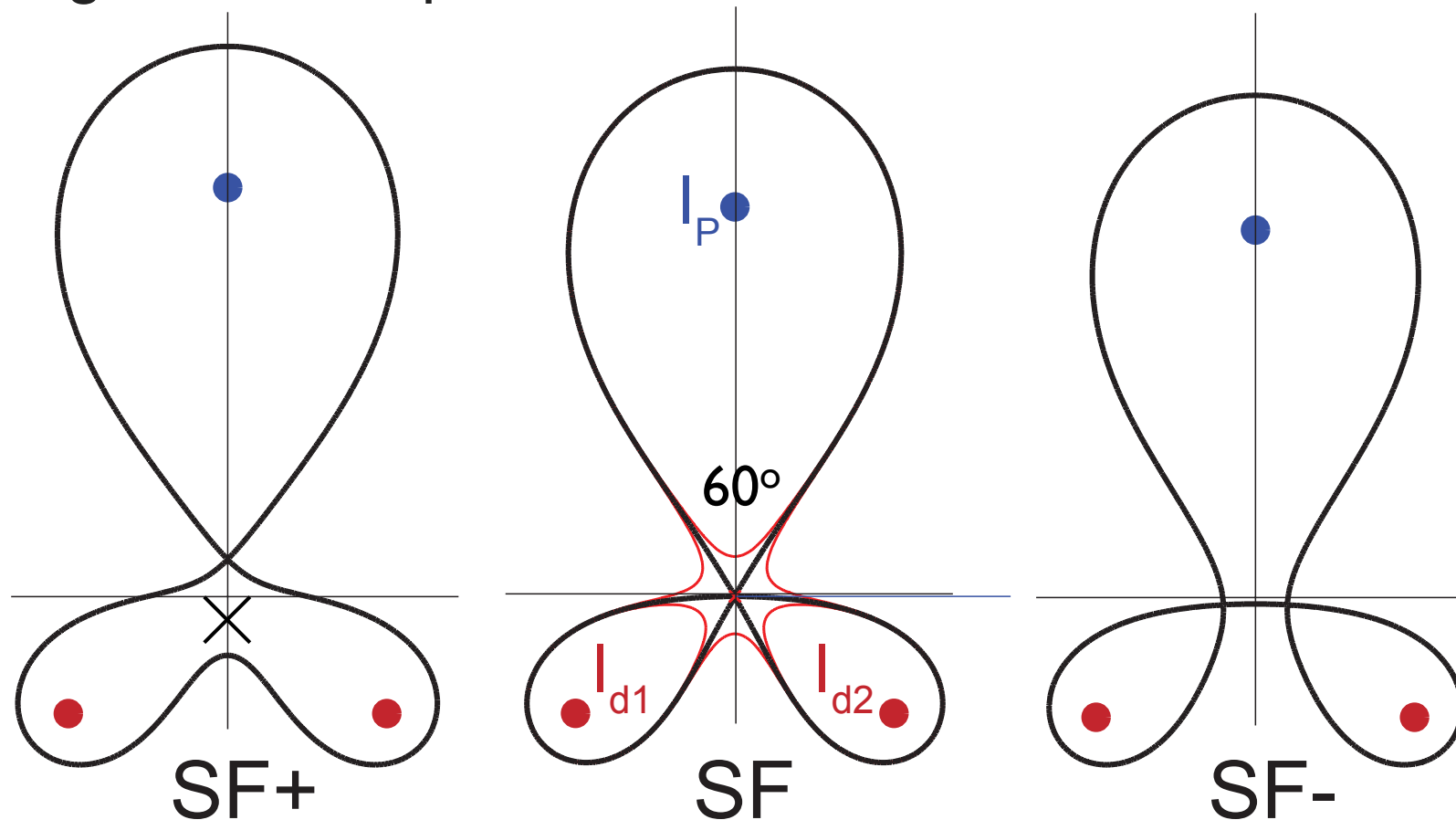
Divertor lifetime remains a crucial issue for tokamaks

- New solutions proposed to reduce the power heat loads:
  - ▶ The Snowflake Divertor [D.D.Ryutov, 2007]
  - ▶ The Super-X Divertor [P.M.Valanju, 2009]

# The Snowflake Divertor Concept

## X-point replaced by second order null

- $B_P = 0$  AND  $\nabla B_P = 0$
- 4 divertor legs
- Minimum two divertor coils necessary
- Separatrix angle at the X-point of  $60^\circ$  instead of  $90^\circ$

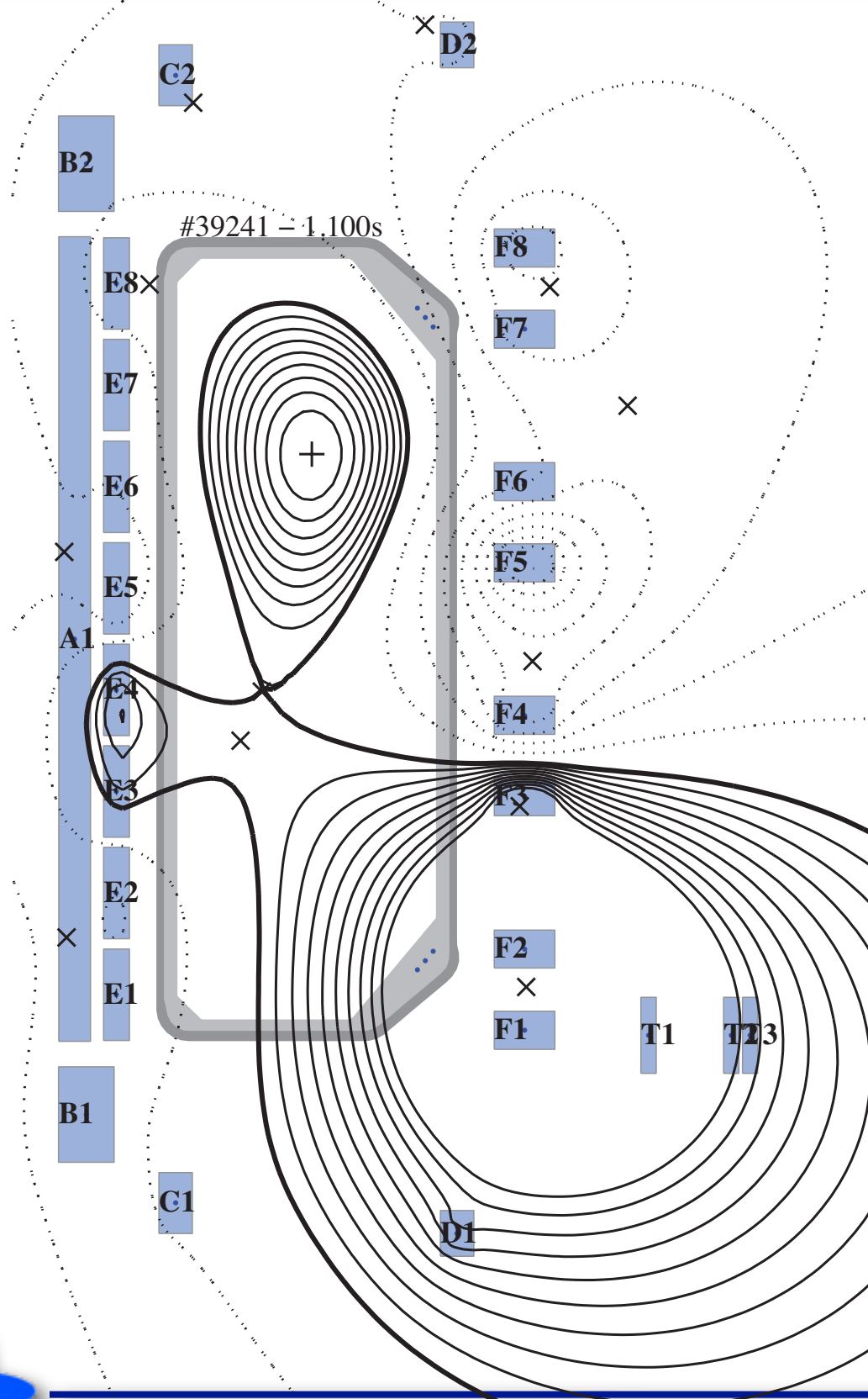


- The SF features:
  - ▶ Larger flux expansion in the X-point region
  - ▶ Longer connection length in the SOL
  - ▶ Higher magnetic shear close to the separatrix

F.Piras, PPCF 2010  
V.Soukhanovskii, APS 2010

# Creating a Snowflake on TCV

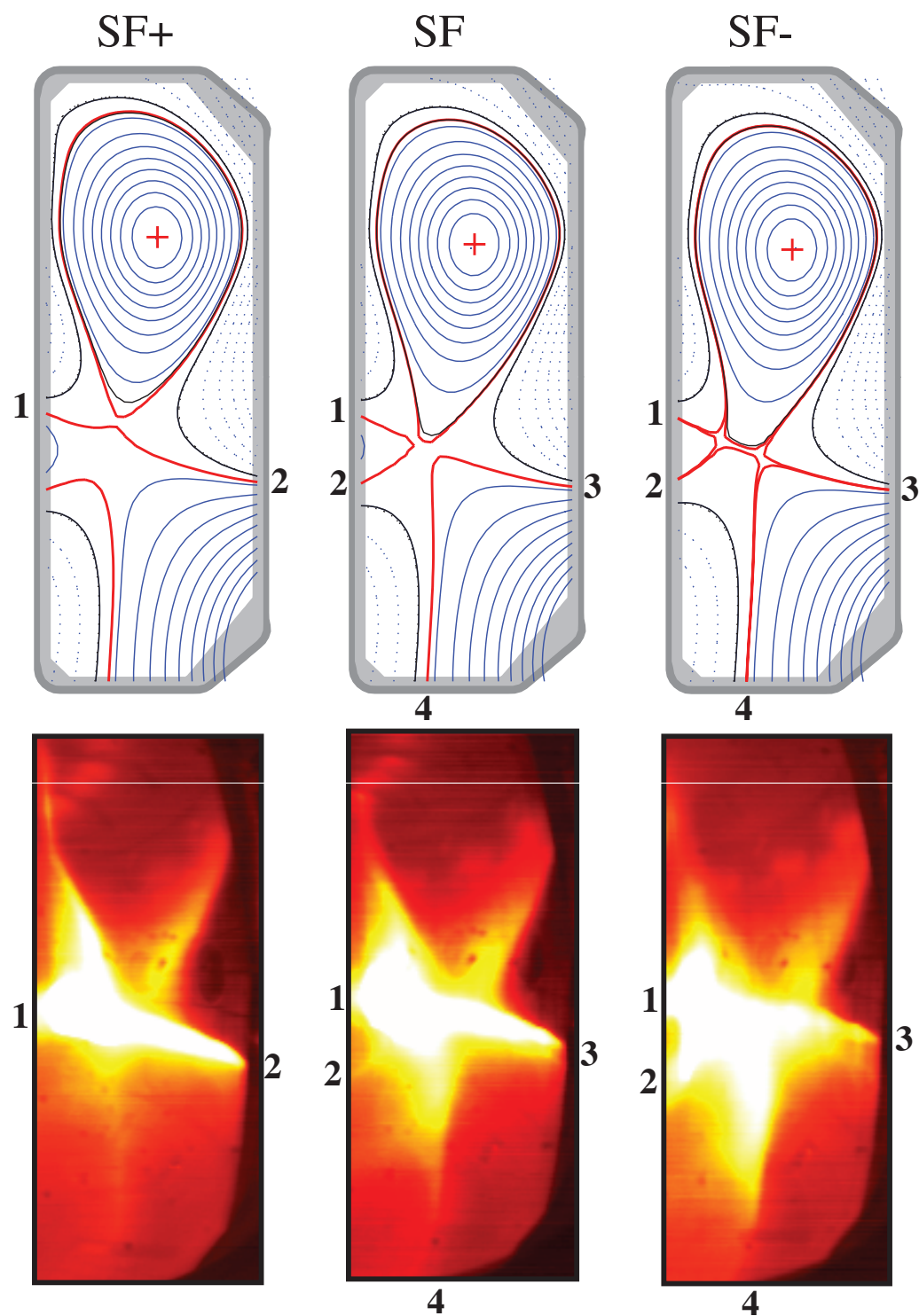
Snowflake Divertor demonstrated for the first time in TCV



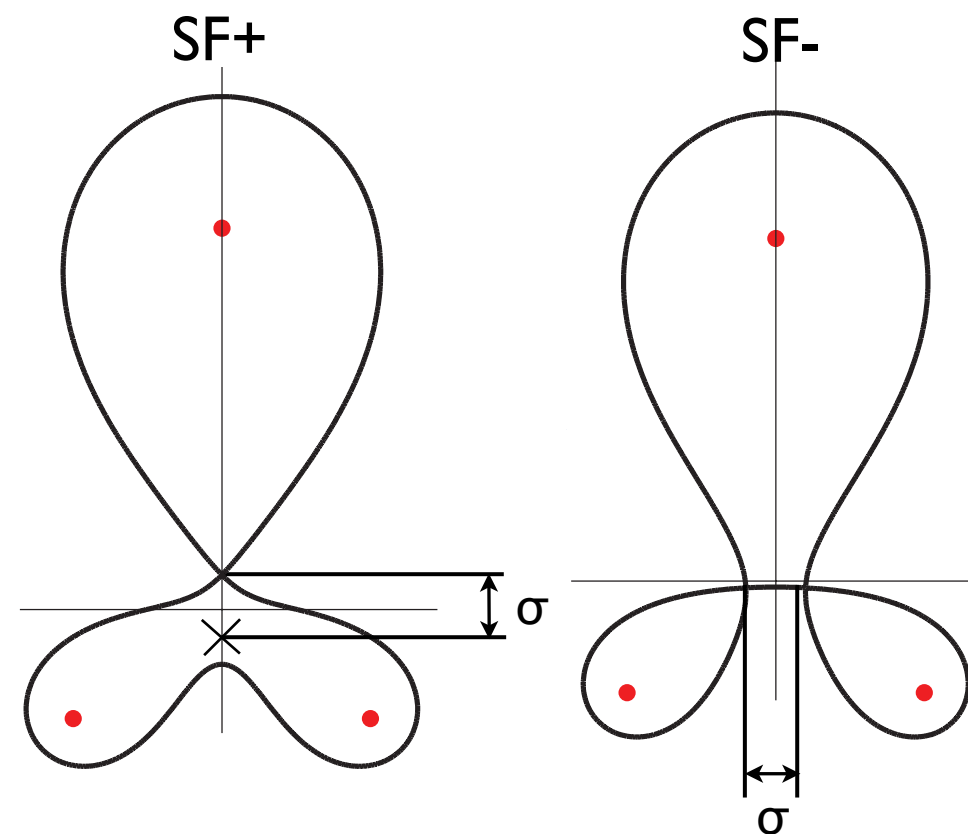
- Open divertor can be freely configured
  - ▶ 16 independently powered coils
  - ▶ Vessel covered with graphite tiles
- Several PF coils used as SF divertor coils

# Viewing a Snowflake on TCV

All three SF configurations have been successfully established and controlled



- ▶ The tangential visible camera confirms the magnetic configurations
- ▶  $\sigma$  parametrizes the proximity to an ideal snowflake configuration (SF)



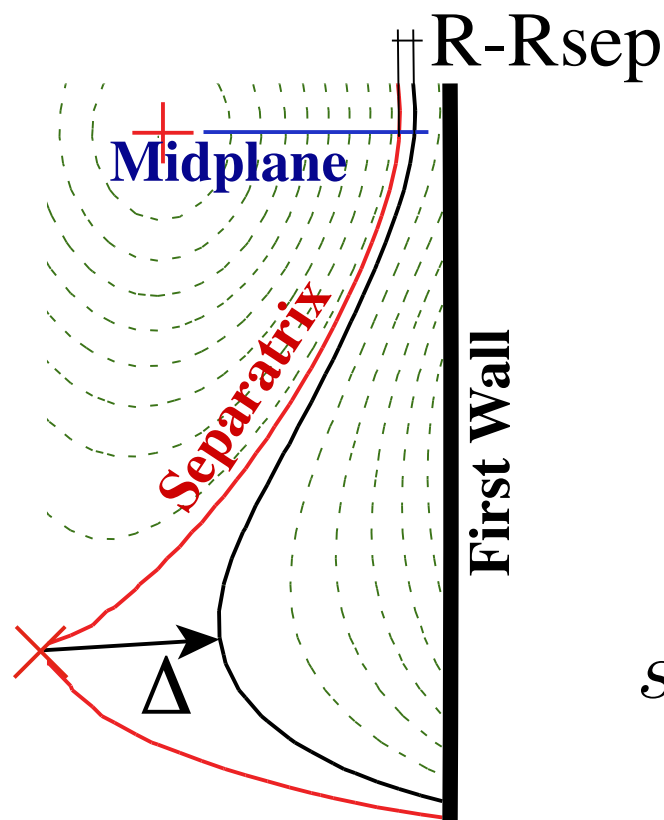
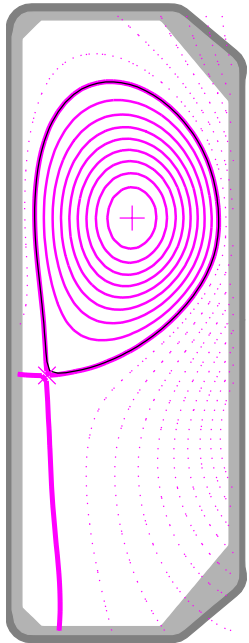
F.Piras, PPCF 2009

# Magnetic Structure of TCV Snowflake

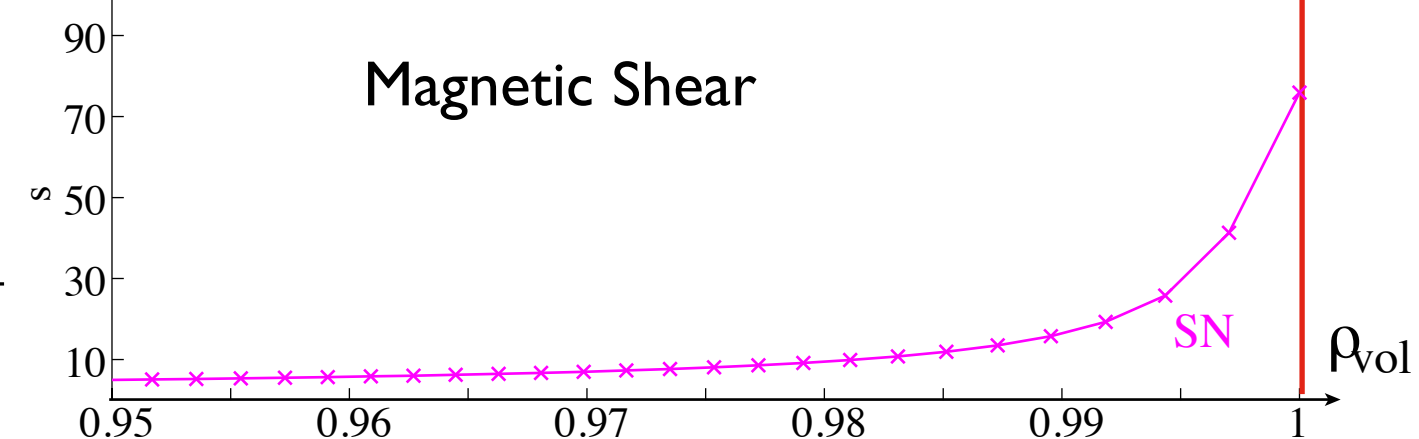
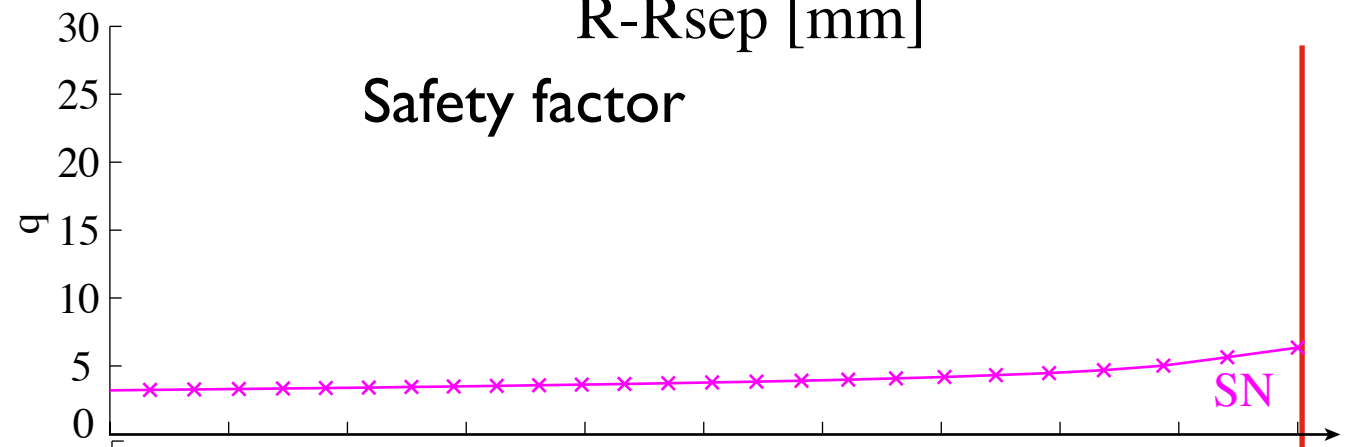
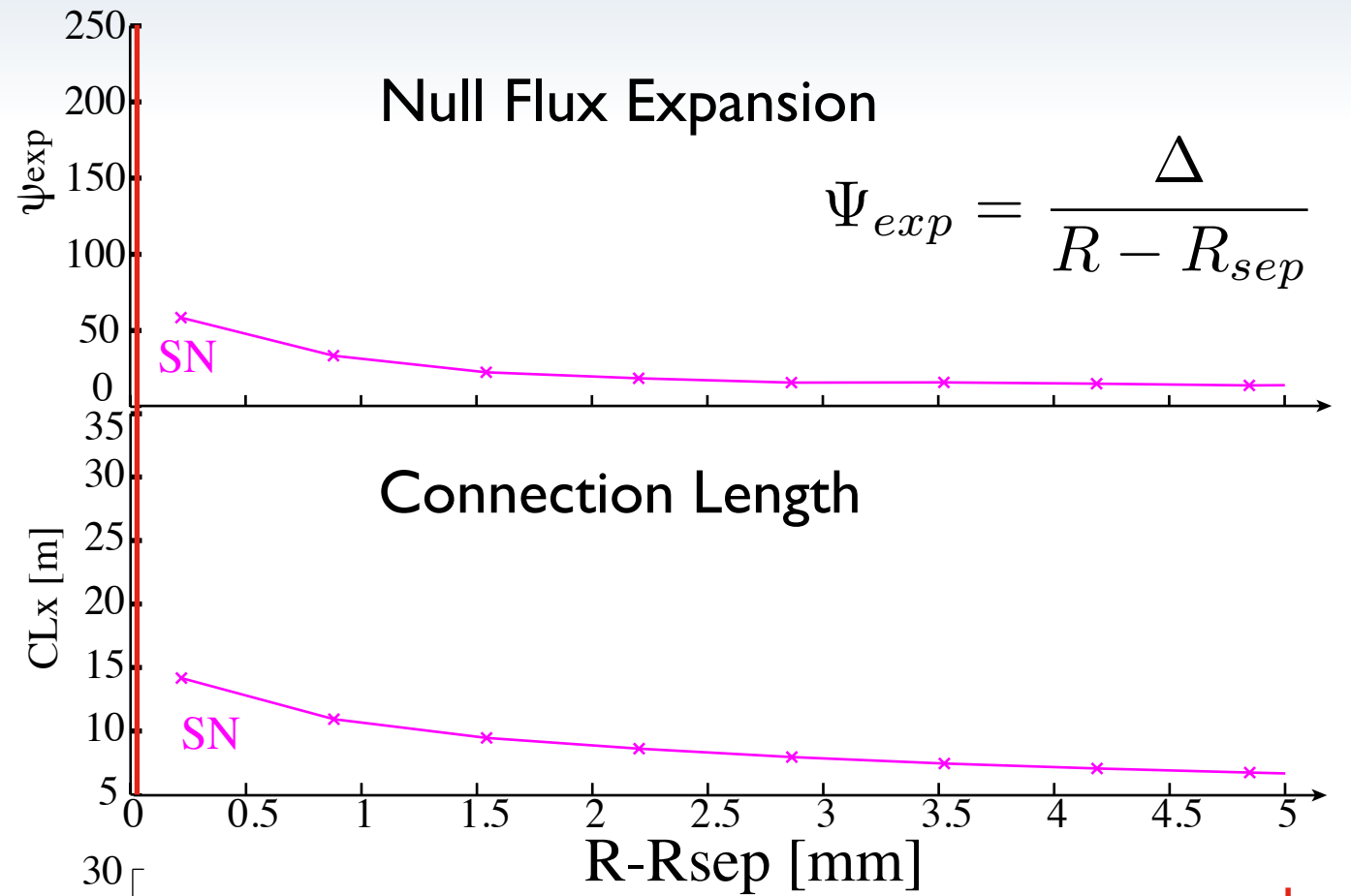
$I_p = 230\text{kA}$ ,  $B_T = 1.4\text{T}$

SN

#35137, 0.6004s



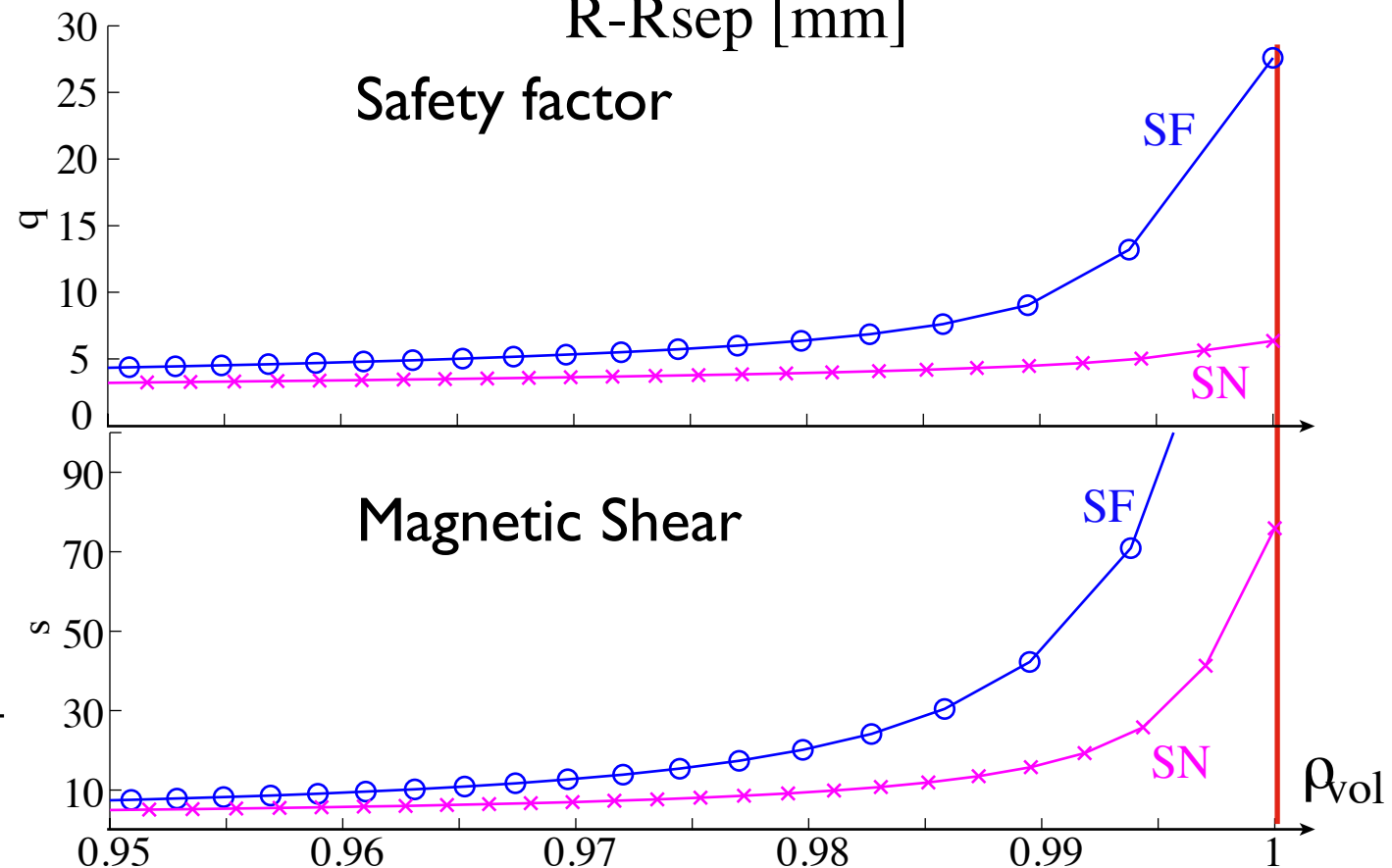
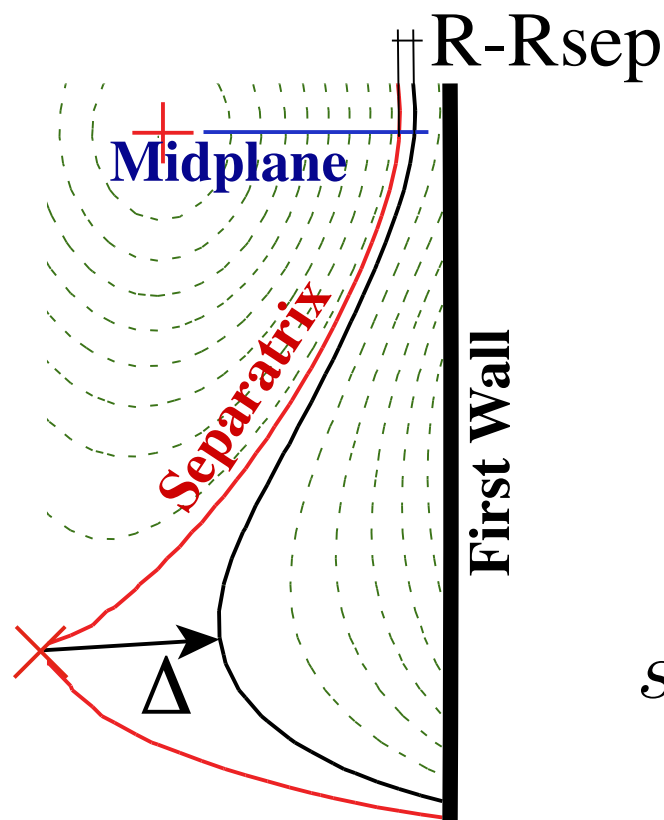
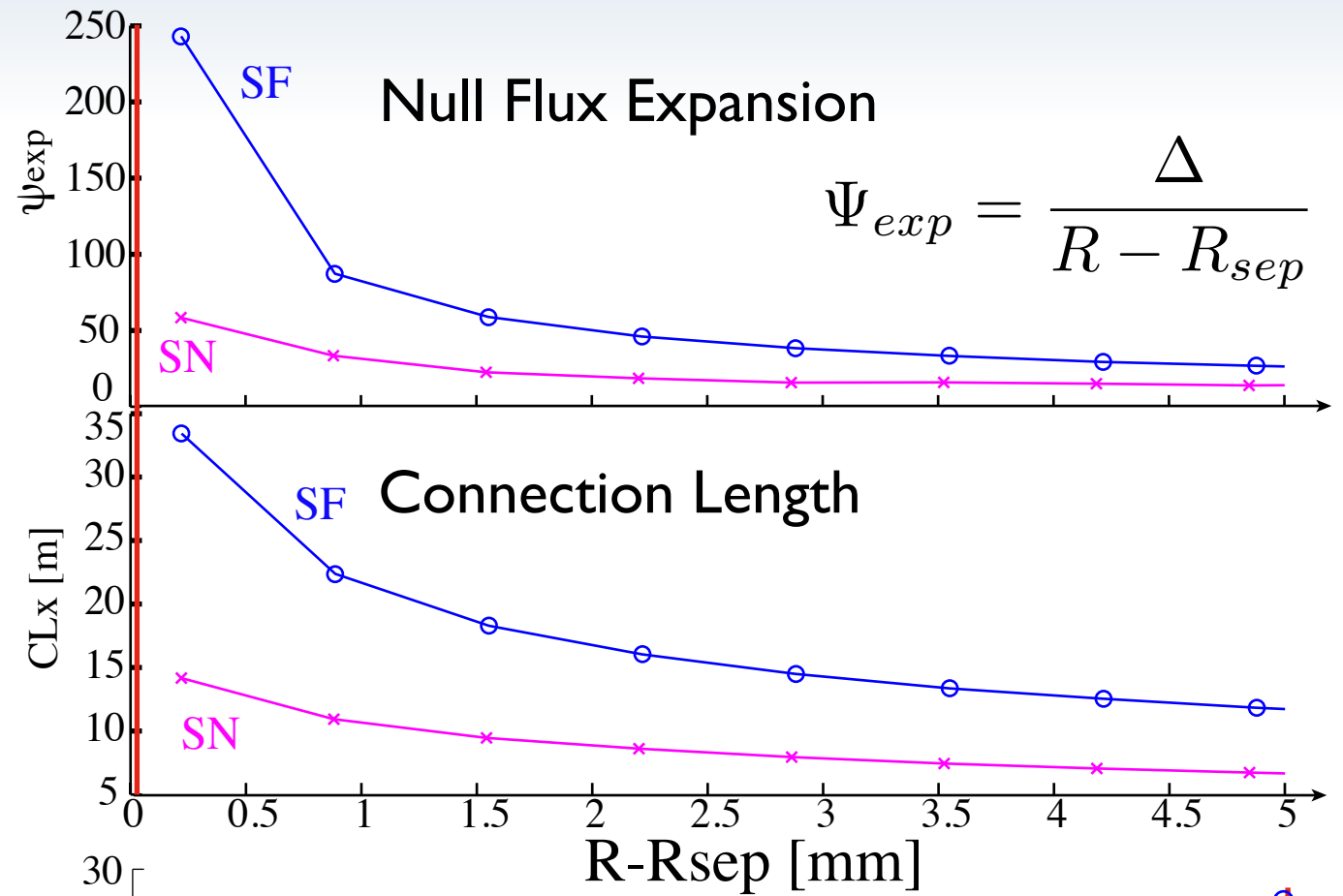
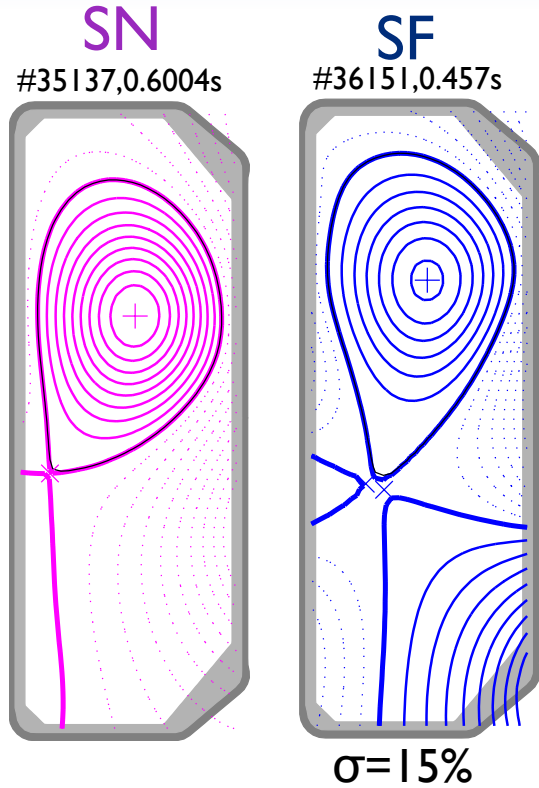
$$s = \frac{\rho_{vol}}{q} \frac{dq}{d\rho_{vol}}$$





# Magnetic Structure of TCV Snowflake

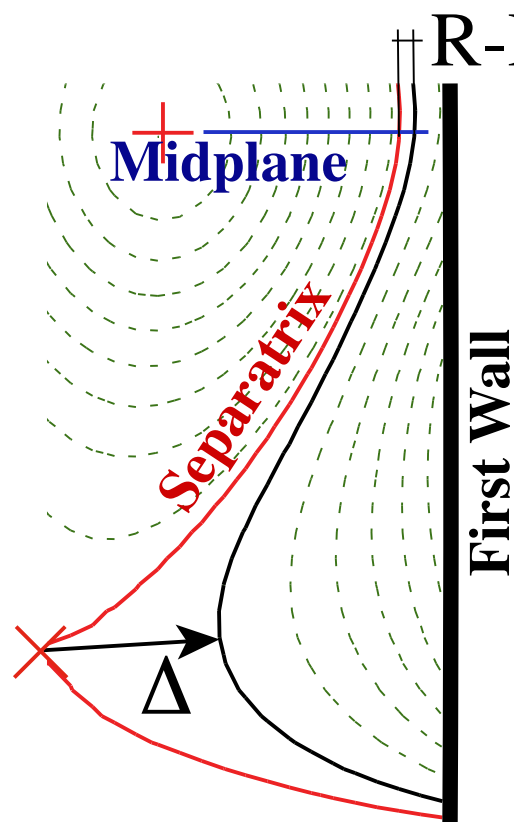
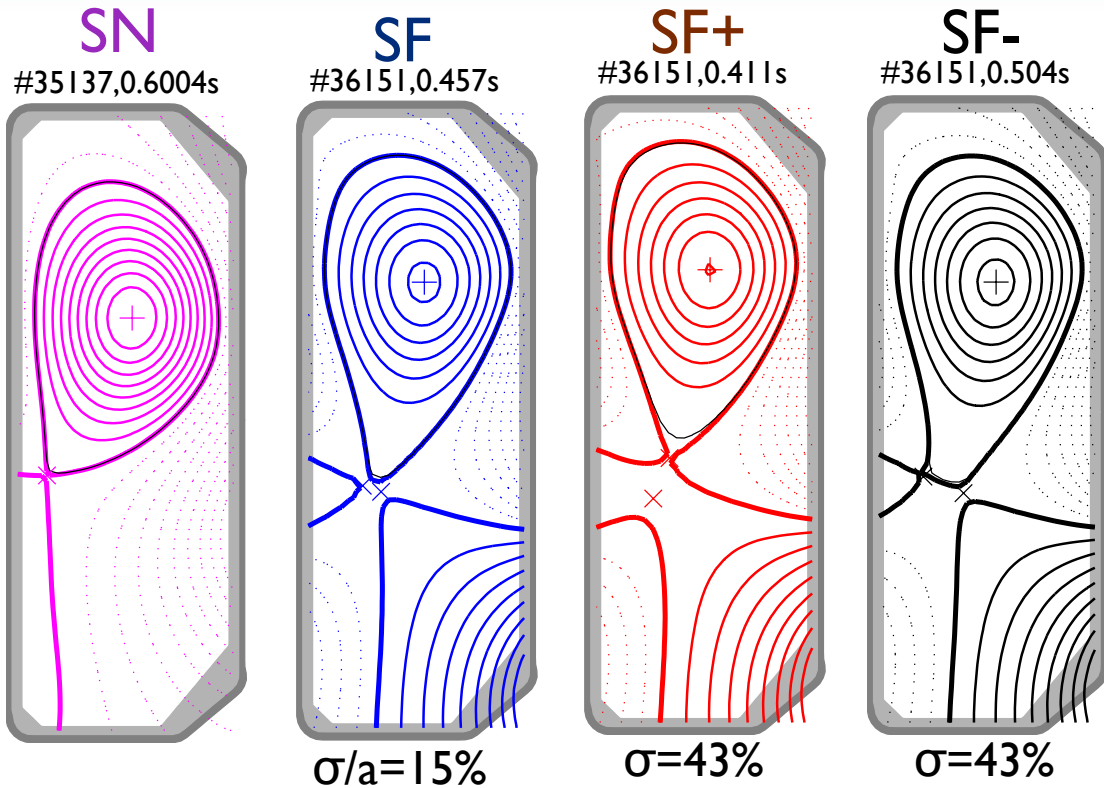
$I_p = 230\text{kA}$ ,  $B_T = 1.4\text{T}$



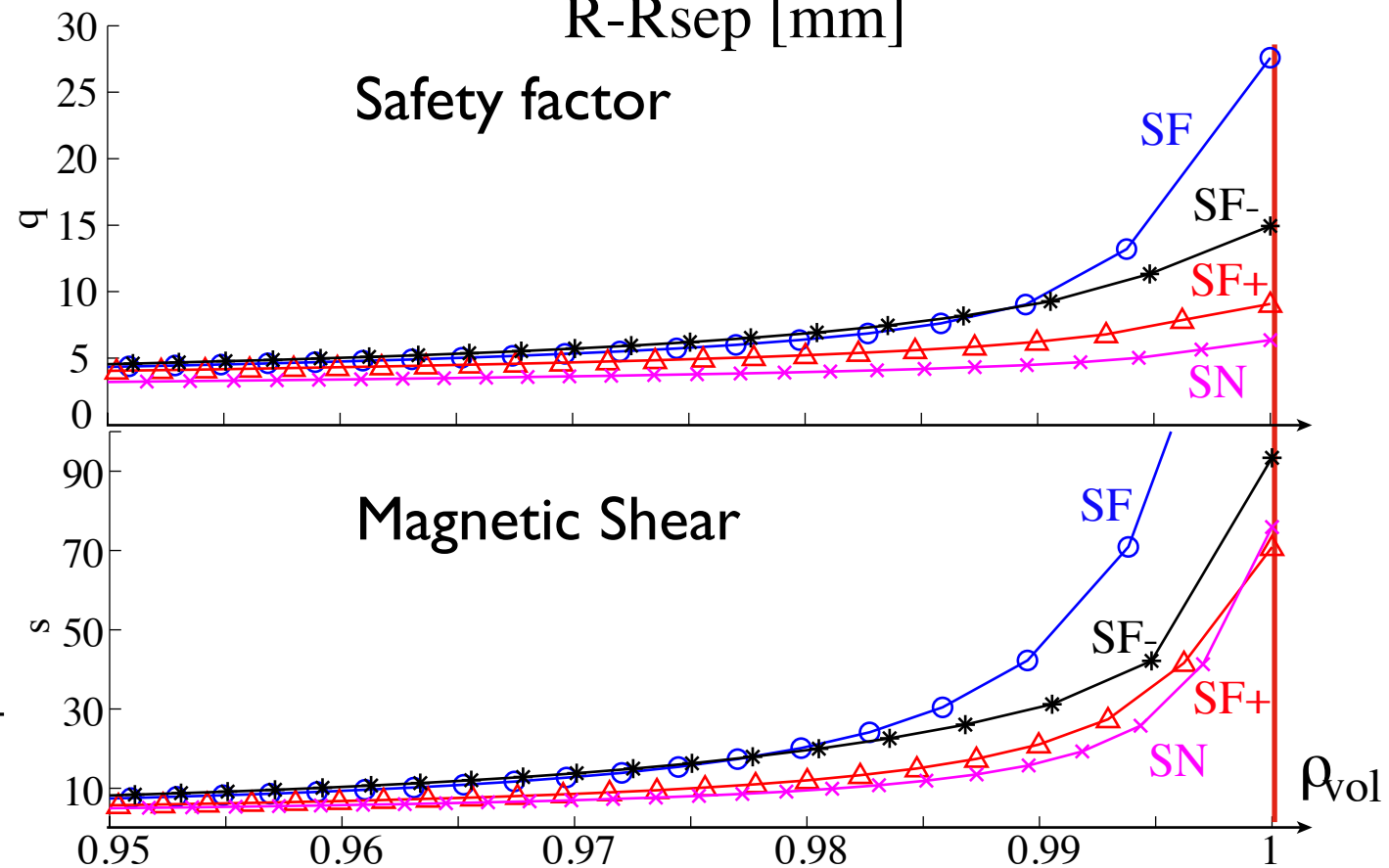
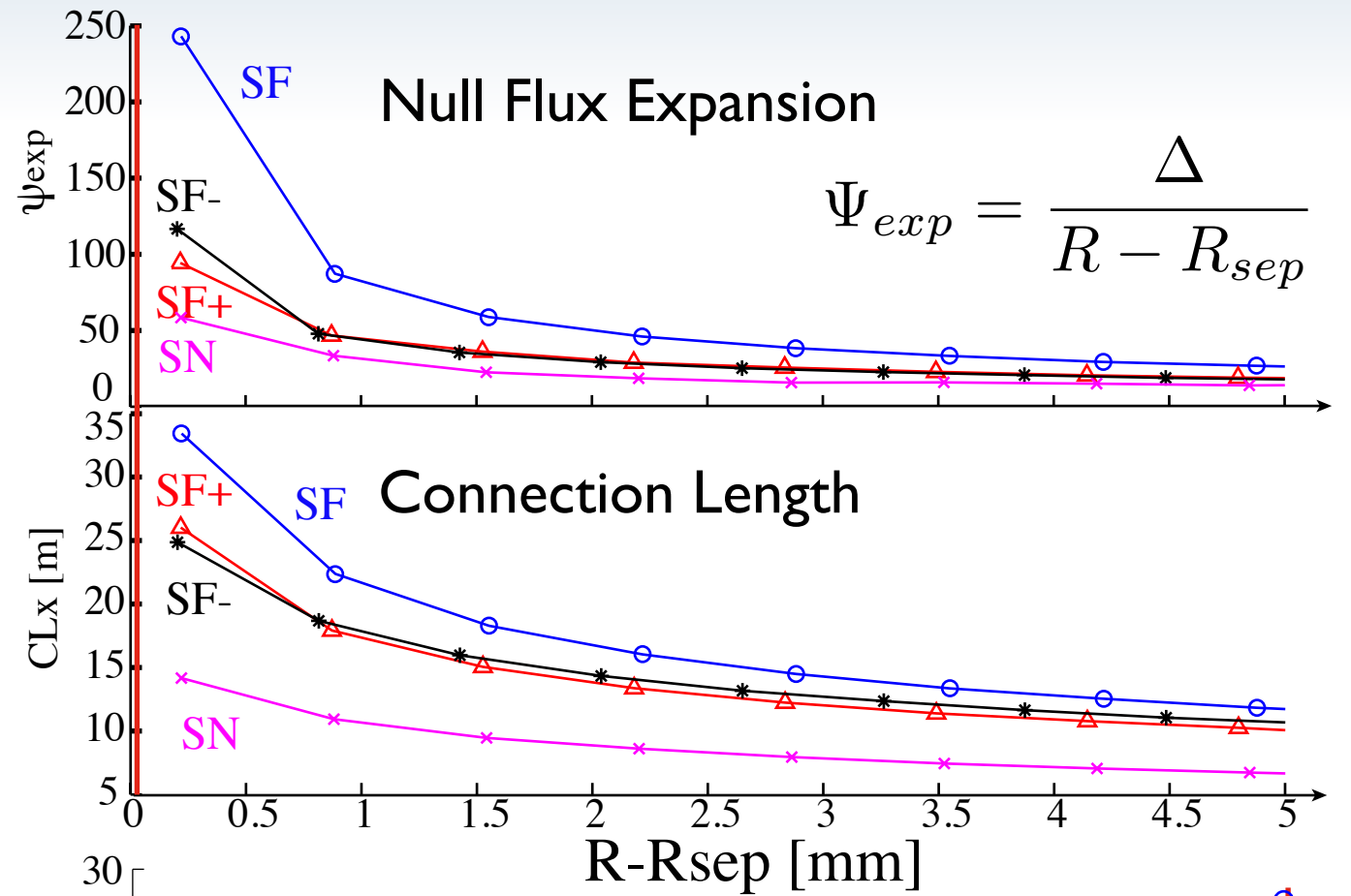
$$s = \frac{\rho_{vol}}{q} \frac{dq}{d\rho_{vol}}$$

# Magnetic Structure of TCV Snowflake

$I_p = 230\text{kA}$ ,  $B_T = 1.4\text{T}$



$$s = \frac{\rho_{vol}}{q} \frac{dq}{d\rho_{vol}}$$



# Exploring H-mode Snowflakes

## Motivation:

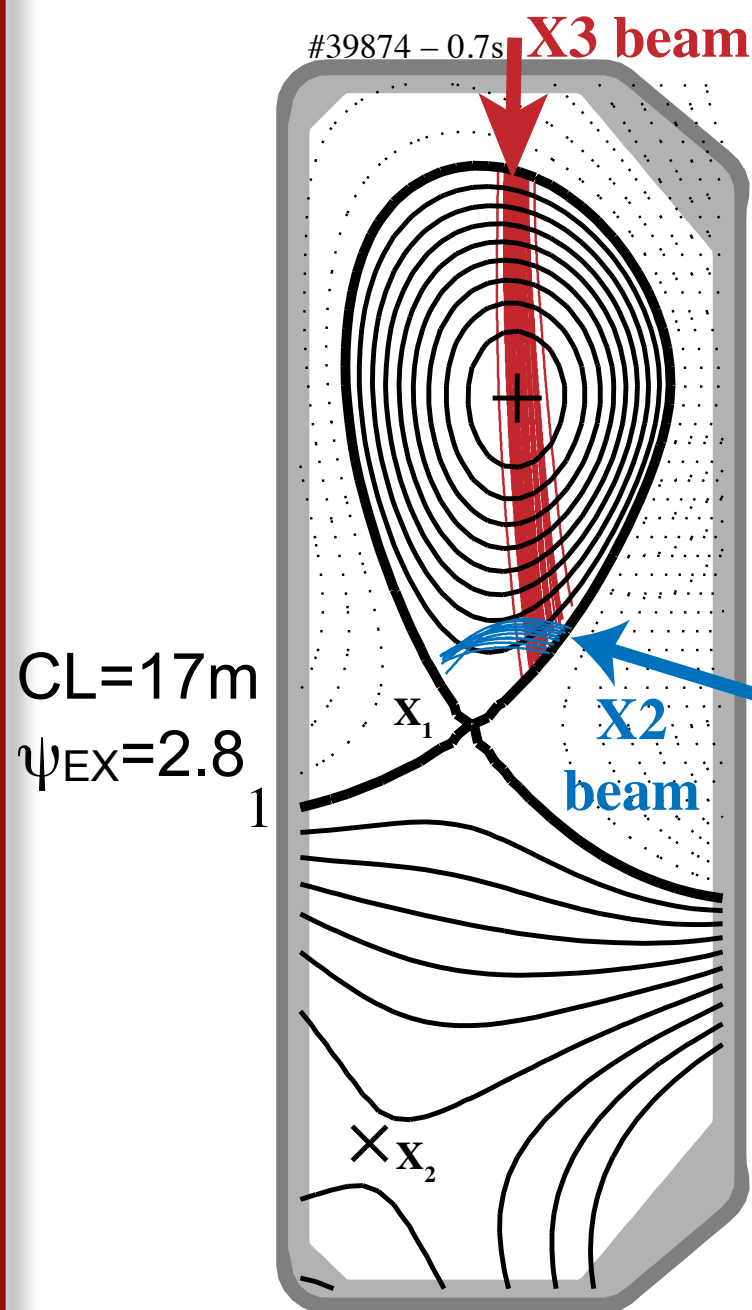
- The H-mode and ELMs are important in present and future tokamaks
- Do the different SF magnetic properties affect the H-mode?

## Experiments:

- Can a SF divertor reach an ELMy H-mode?
- How do the ELM dynamics compare with a SN H-mode?
- Can we channel ELM power onto the additional strike points?

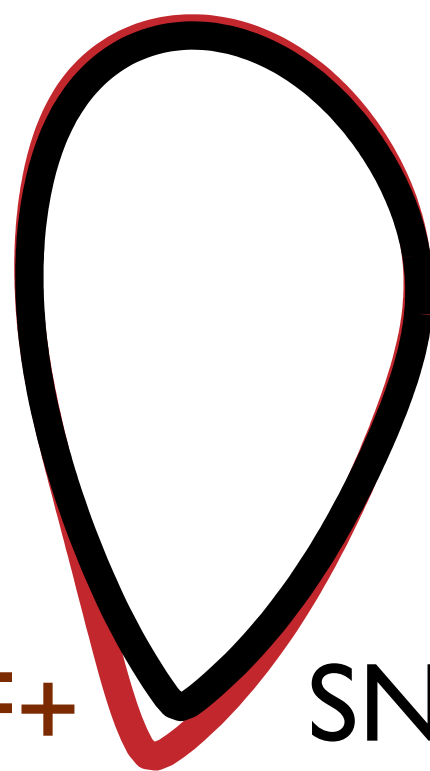
# Tuning the Configurations

Comparison between SN and SF+ with similar plasma shape

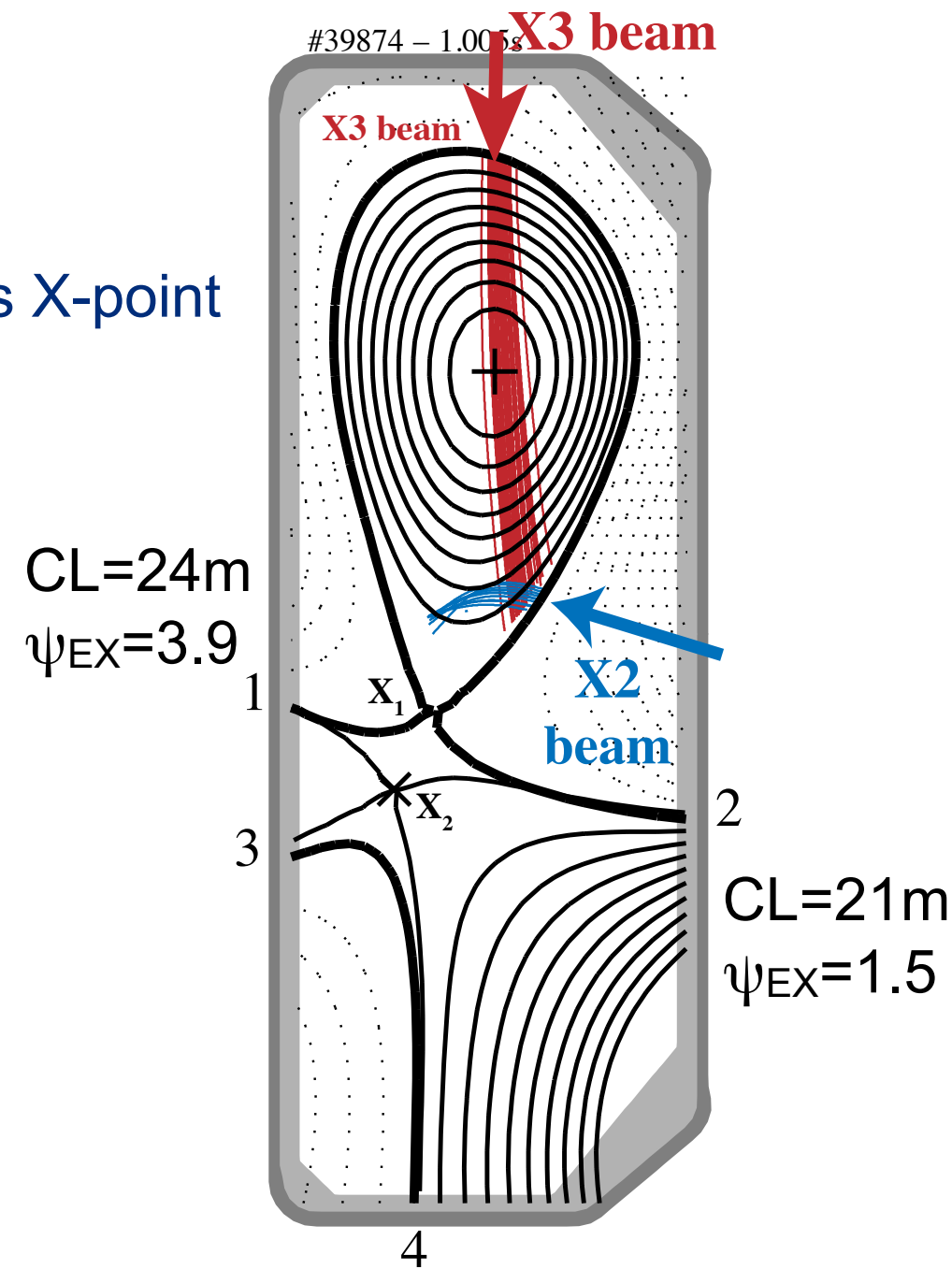


SN  $\sigma=270\%$

- Plasma properties
  - ▶  $I_p = 300\text{kA}$
  - ▶  $B \times \nabla B$  ion-drift towards X-point
- Additional heating
  - ▶ 1MW ECH-X3
  - ▶ 0.5-1MW ECH-X2



SF+ SN

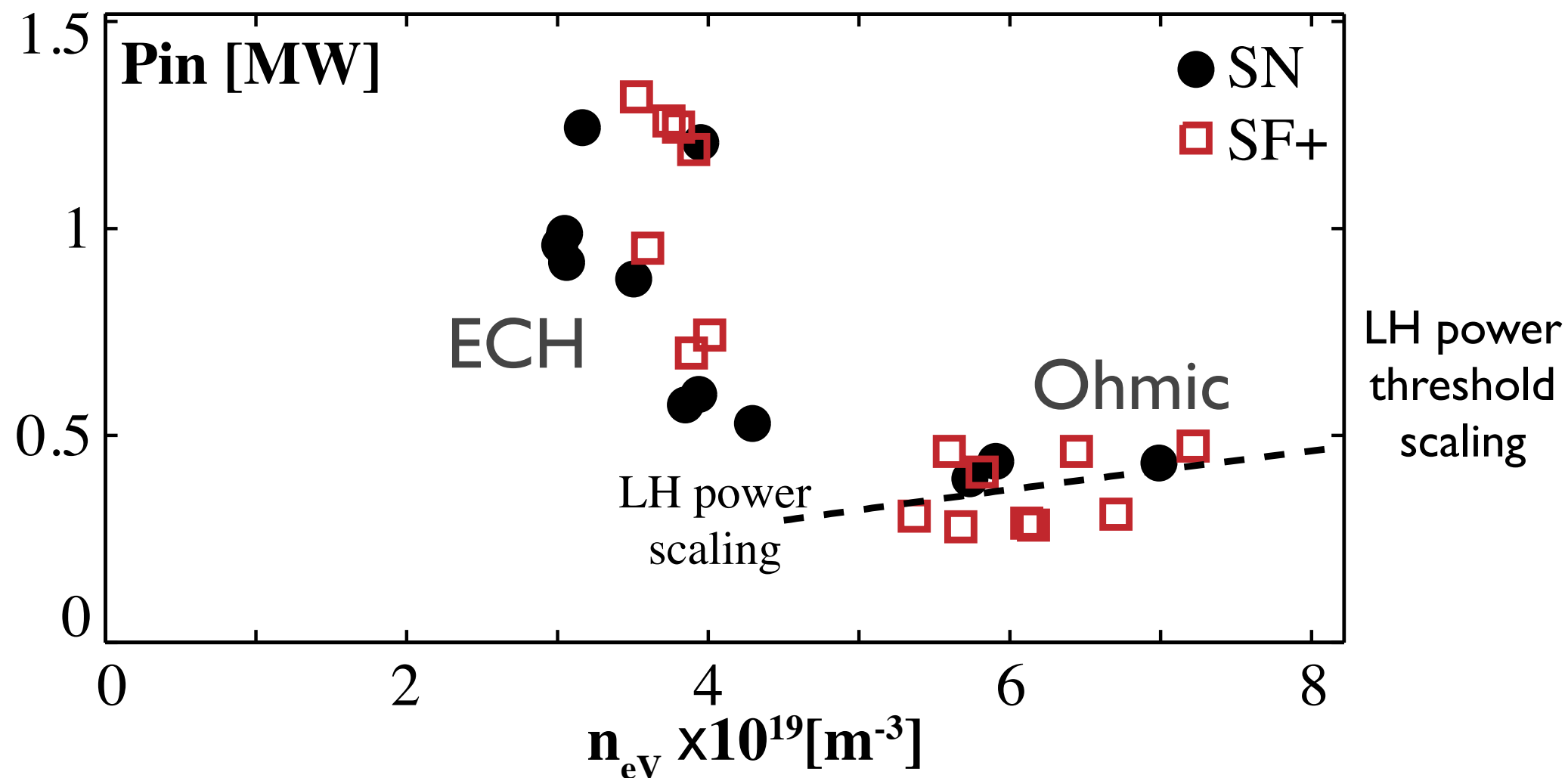


SF+  $\sigma=55\%$



# Accessing the H-mode

## Comparison SN and SF+



- Scan  $P_{in}$  to identify H-mode power threshold
  - ▶ Low density: a fraction of  $P_{in}$  from ECH
  - ▶ High density: only ohmic power (ECH cut-off)

**Unchanged power threshold for Ohmic and ECH H-modes**

# Type I ELMy H-mode

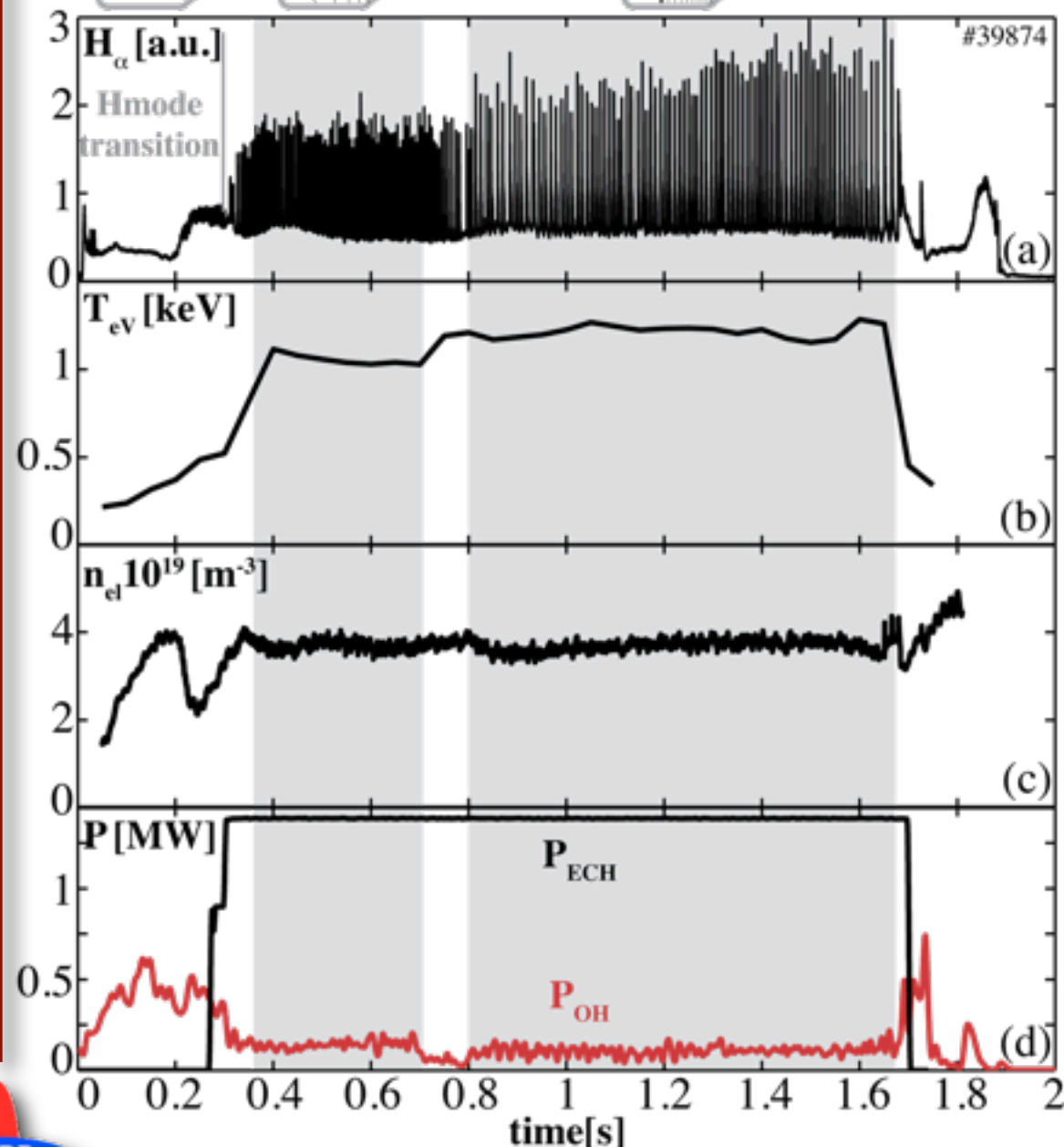
## ELMy H-mode for SN and SF+ within the same discharge



- SF+ established from SN moving the second X-point toward the SN X-point

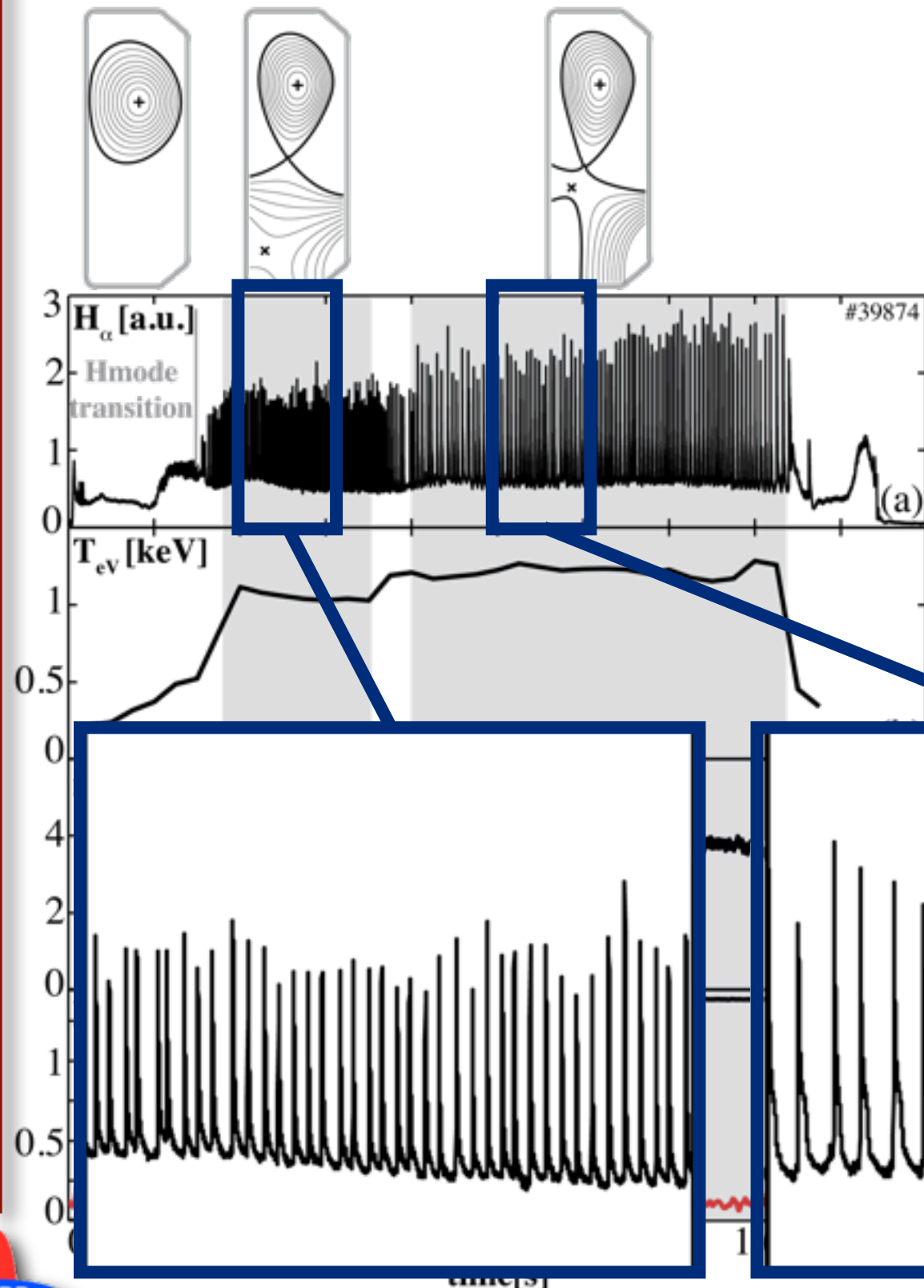
- After the transition:

- ▶  $T_e$  and confinement increase by  $\sim 15\%$
- ▶ The ELM frequency is lower
- ▶ H $\alpha$  spikes and integrated H $\alpha$  across each ELM increase by  $\sim 30\%$



# Type I ELMy H-mode

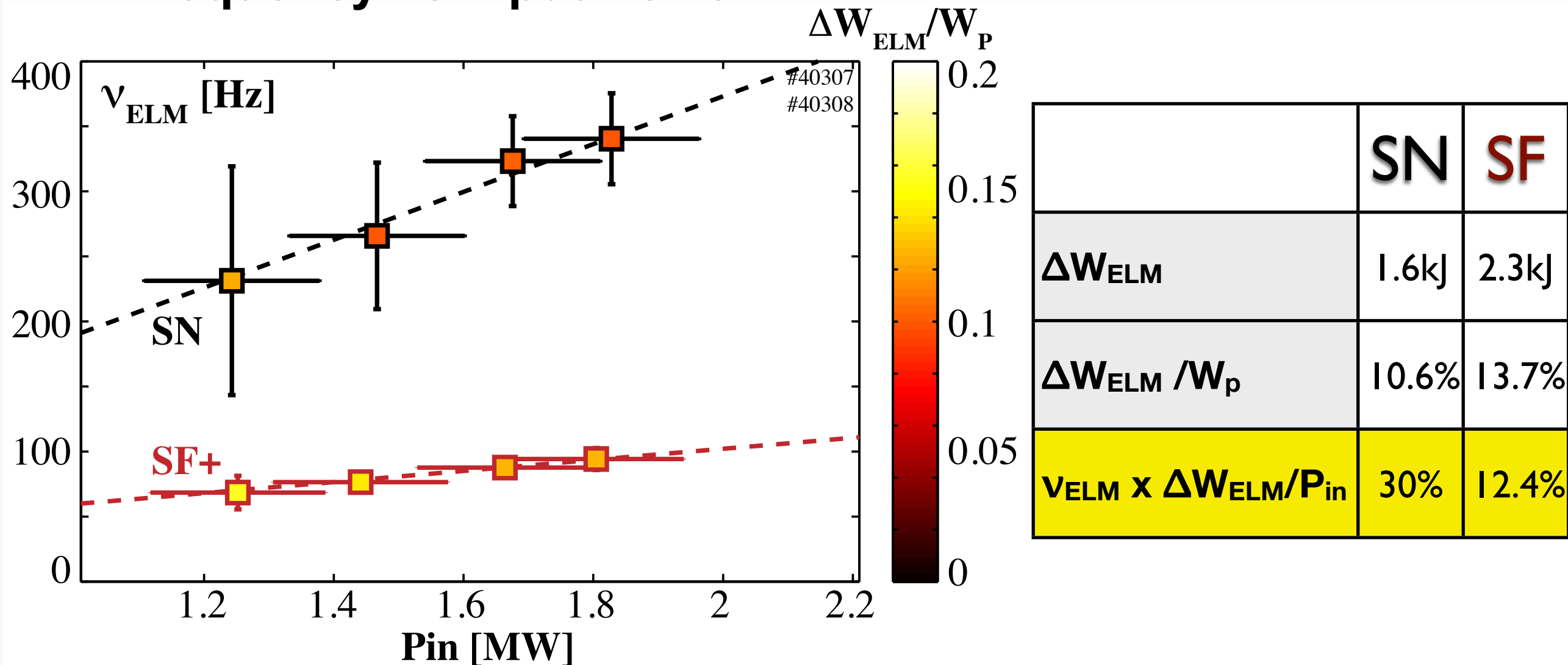
## ELMy H-mode for SN and SF+ within the same discharge



- SF+ established from SN moving the second X-point toward the SN X-point
- After the transition:
  - ▶ T<sub>e</sub> and confinement increase by ~15%
  - ▶ The ELM frequency is lower
  - ▶ H<sub>α</sub> spikes and integrated H<sub>α</sub> across each ELM increase by ~30%

# Snowflake Reduces ELM Frequency

## ELM Frequency vs Input Power

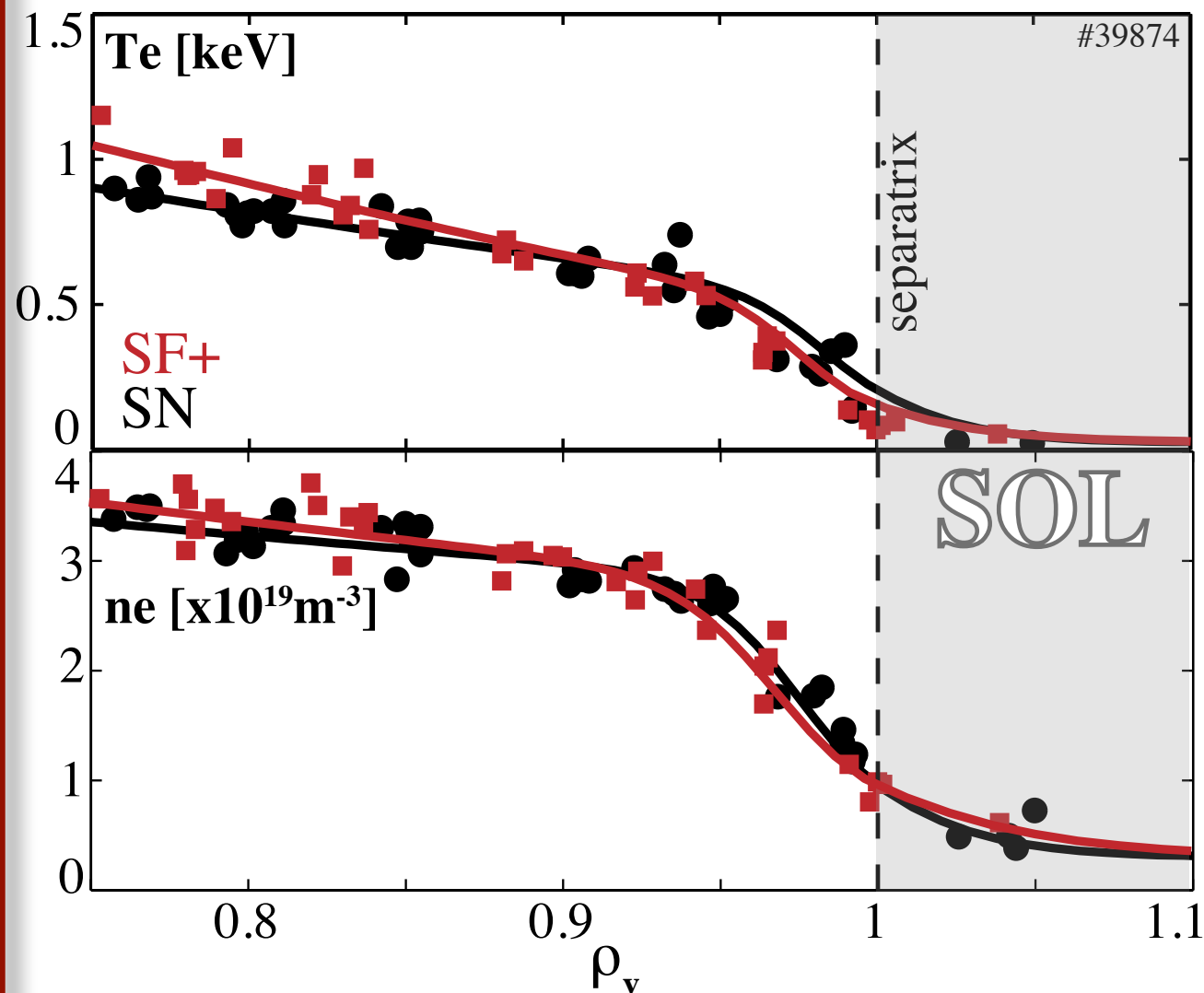


- Scan ECH-X2 input power keeping ECH-X3 constant
- $d\nu_{ELM}/dP_{in} > 0$  for both configurations  $\rightarrow$  type I ELMs
- SF+ has 2-3 times lower  $\nu_{ELM}$
- $\Delta W_{ELM}/W_P$  only 20-30% higher in SF+
- $\nu_{ELM}$  does not change with X2/X3 deposition,  $\kappa$ , SF+  $\rightarrow$  SN

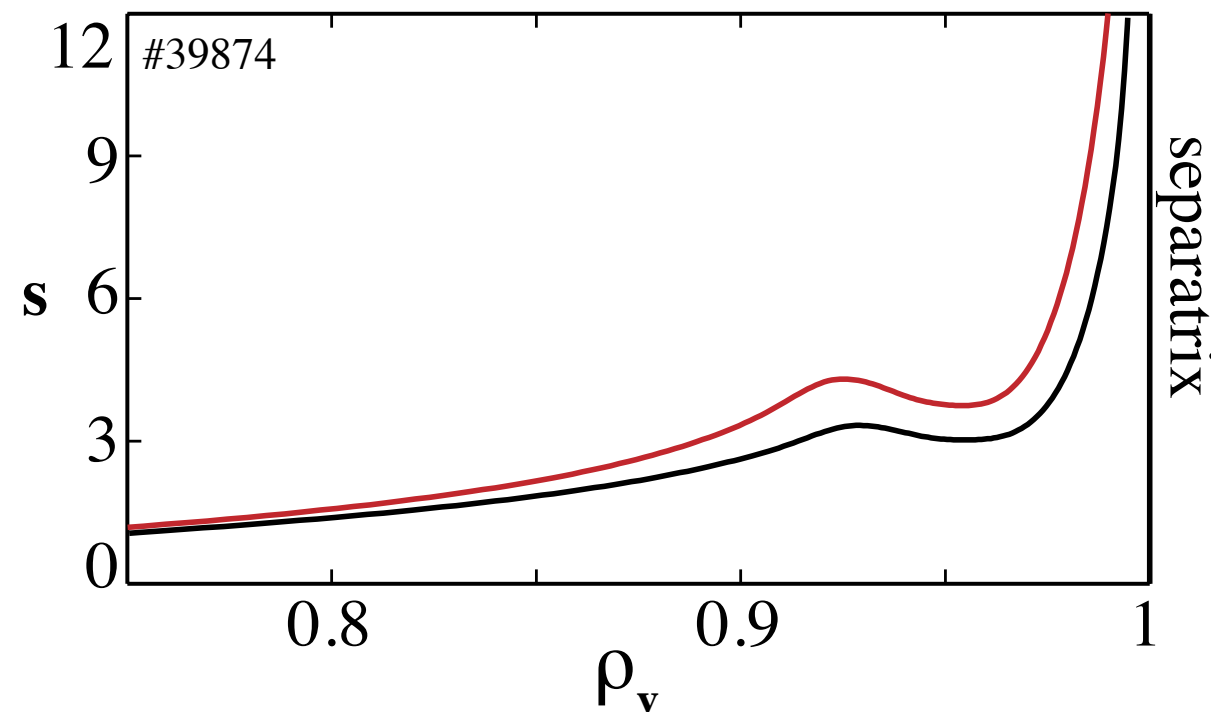


# Similar Pedestal Profiles

## Temperature and density profiles



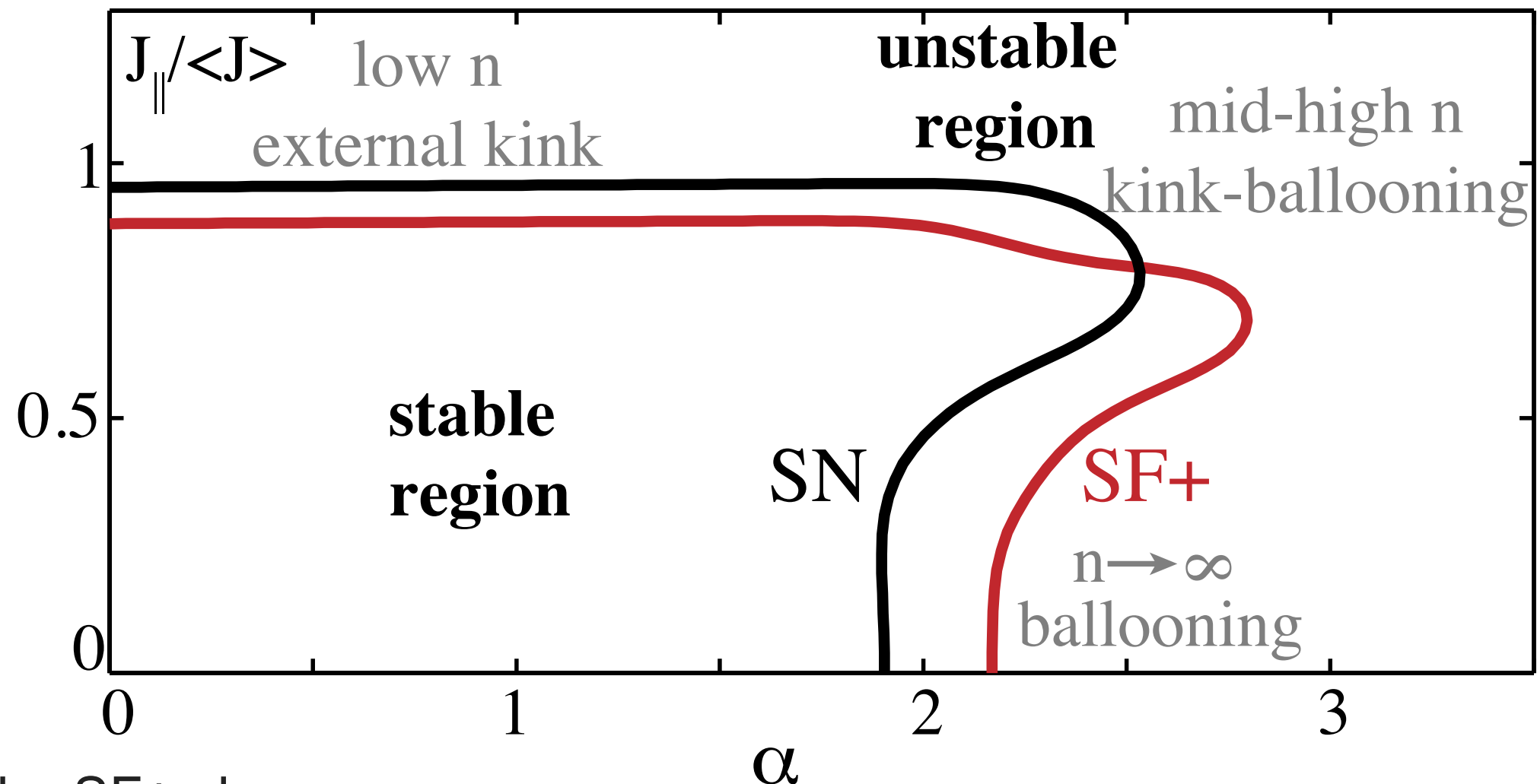
- Similar  $T_e$  and  $n_e$  profiles from Thomson scattering



- Magnetic shear includes the bootstrap current
- SF+ has higher magnetic shear

# Enhanced Pedestal Stability

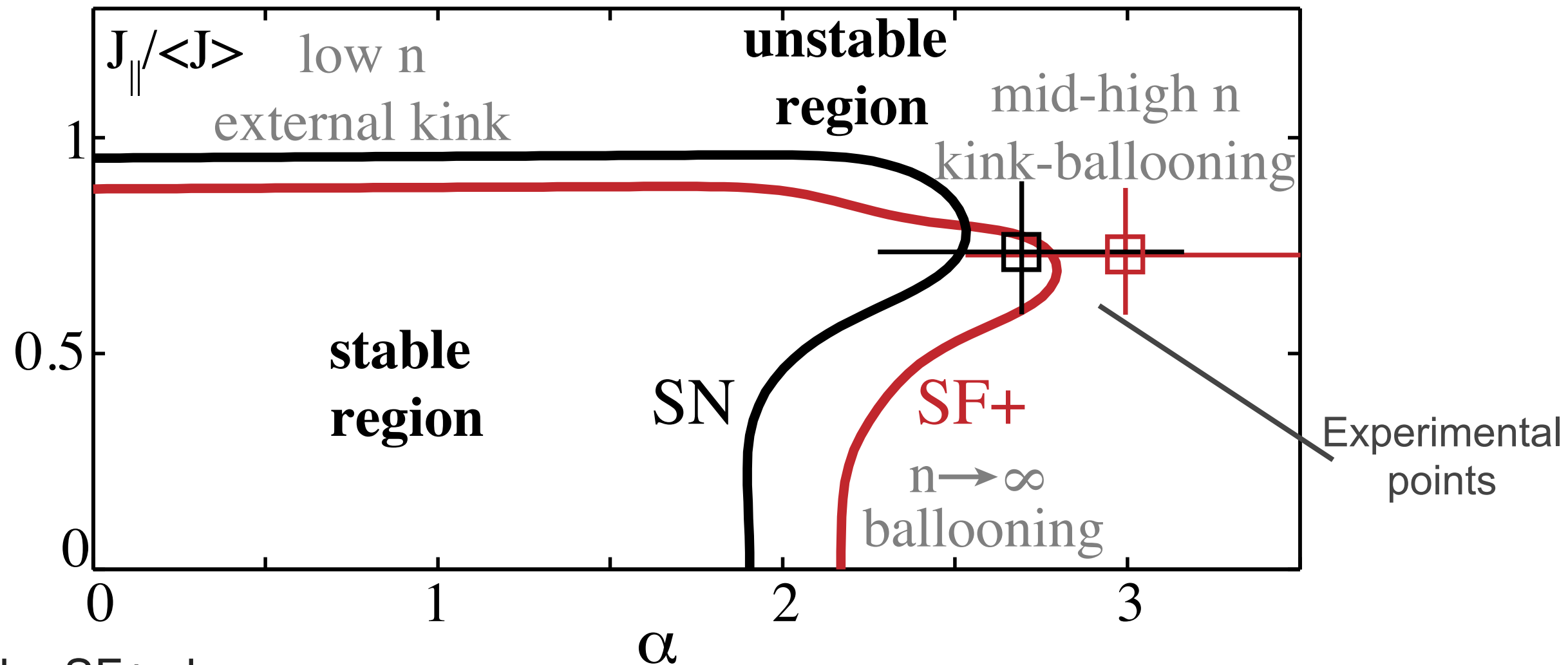
Ideal MHD pedestal stability computed with the KINX code



- The SF+ shows:
  - ▶ Larger second stability region, i.e. enhanced kink-ballooning stability
  - ▶ Better stability of ideal ballooning modes ( $n \rightarrow \infty$ )
  - ▶ Lower low n (external kink) stability limits

# Enhanced Pedestal Stability

Ideal MHD pedestal stability computed with the KINX code

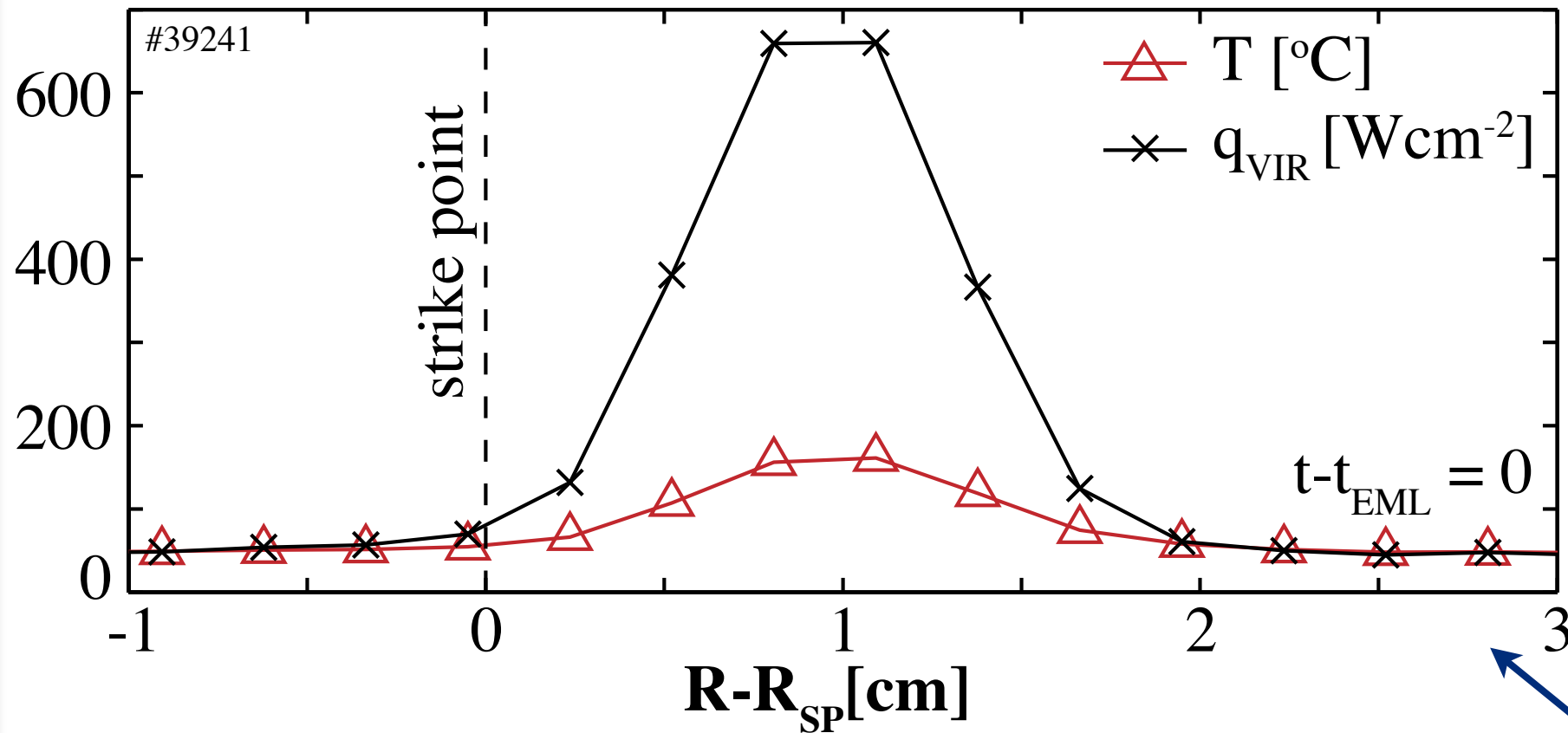


- The SF+ shows:
  - ▶ Larger second stability region, i.e. enhanced kink-ballooning stability
  - ▶ Better stability of ideal ballooning modes ( $n \rightarrow \infty$ )
  - ▶ Lower low n (external kink) stability limits

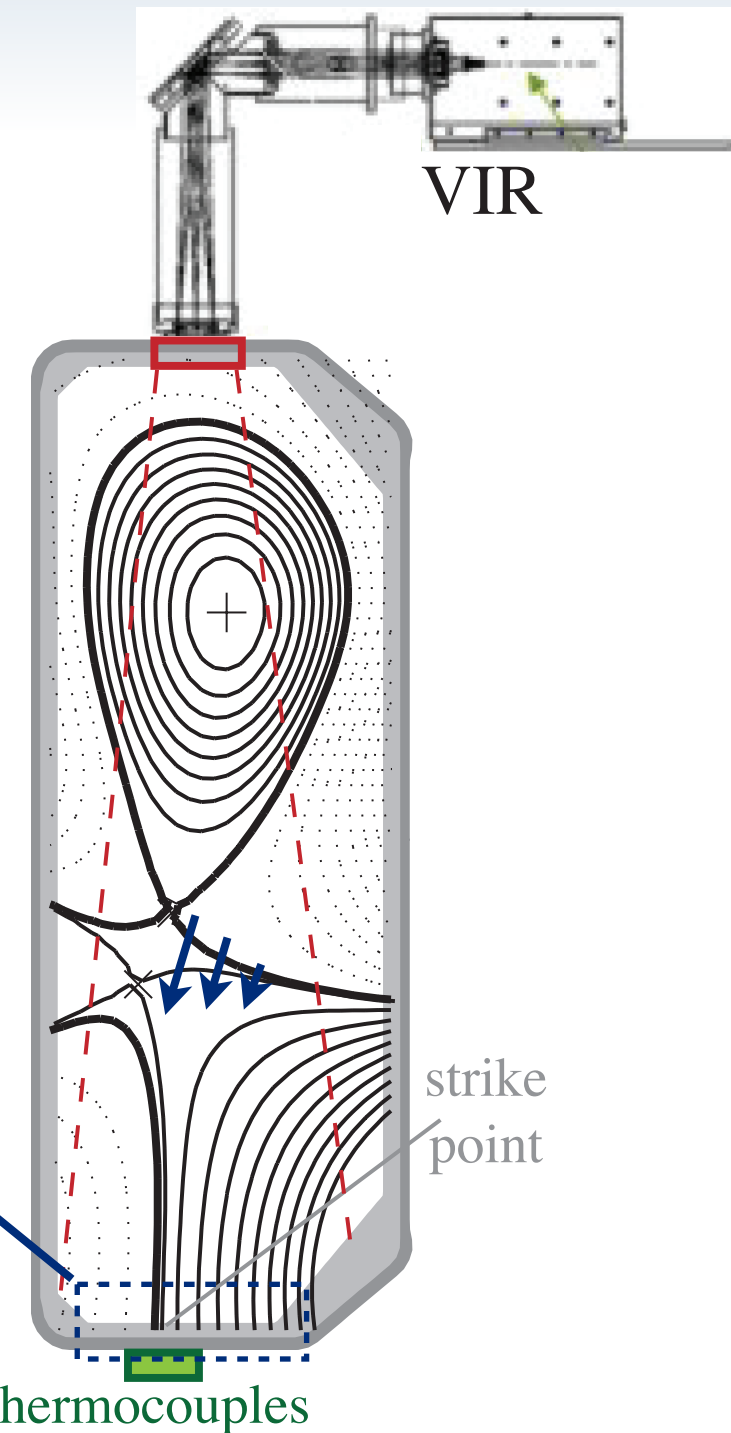
# Strike Point Power Sharing

## Vertical infrared camera profiles

- Coherently averaged ELM profiles



- 15% of  $\Delta W_{\text{ELM}}$  reaches the bottom strike point
  - ▶ confirmed with thermocouples on divertor tiles
- Cross-field transport from the null region explains the measured profiles
- No significant profile broadening during ELMs



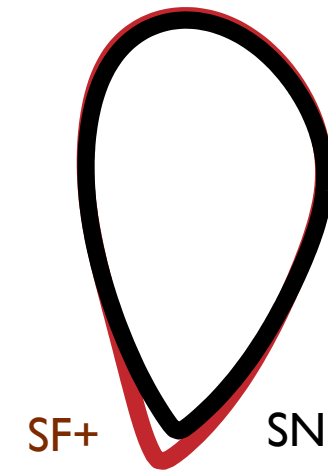
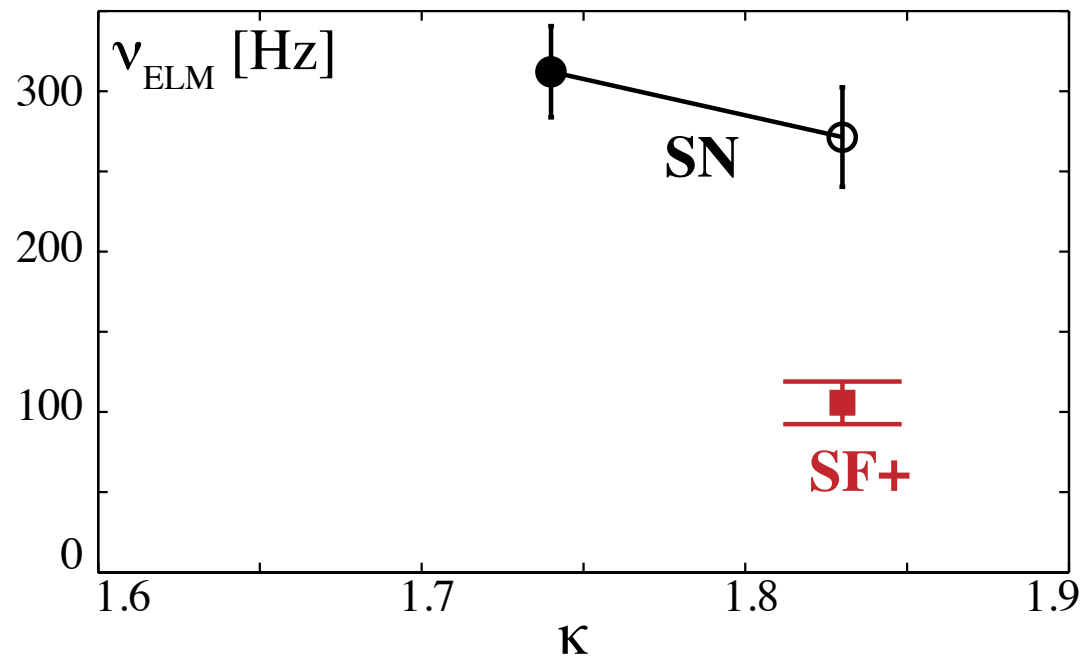
# Conclusions (Snowflake Divertor)

- The snowflake divertor has been established and controlled on TCV with:
  - ▶ Higher flux expansion, connection length and magnetic shear
- An ELMy Type I H-mode was established, showing:
  - ▶ Similar H-mode power threshold to single-null plasmas
  - ▶ ELM frequency reduced by 2-3, while energy lost per ELM increased by 20-30%
  - ▶ Higher plasma temperature and better confinement (~15%)
  - ▶ Similar pedestal profiles
- 15% of the ELM energy reaches one of the additional strike points
- The pedestal stability analysis suggests enhanced kink-ballooning stability
- Future work will focus on the strike point power sharing



# $\nu_{ELM}$ vs X2/X3 absorption, $\kappa$

- $\nu_{ELM}$  does not change with X3 deposition location
- Relatively small variation of  $\nu_{ELM}$  with  $\kappa$



- $\nu_{ELM}$  does not change with X2 deposition location

